Sustainable Food Technology

REVIEW

View Article Online
View Journal | View Issue

Cite this: *Sustainable Food Technol.*, 2024, 2, 307

Starch-based edible packaging: rheological, thermal, mechanical, microstructural, and barrier properties – a review

Ravichandran Santhosh,[b] Jasim Ahmed, *[a] Rahul Thakur[b] and Preetam Sarkar[b]

The alarming adverse impacts of fossil fuel-based packaging materials led to the development of sustainable packaging materials from renewable sources that are readily biodegradable. To reduce the burden of packaging material's end-use, edible packaging in the form of films and coatings is a promising alternative to protect fresh food by maintaining quality and safety, and it can also be used as a delivery vehicle for essential nutrients. Starch, a widely explored plant polysaccharide, might be the best candidate on the list of biodegradable materials due to its natural abundance, thermoplasticity, and, above all, inexpensiveness. However, starch exhibits some limitations as a stand-alone film material, such as inferior barrier and mechanical properties compared to its commercial plastic counterparts. Various approaches have been employed to make it viable for industrial adaptations, including plasticization, co-biopolymer blending, and the incorporation of active additives and nanomaterials. Accordingly, the effect of such strategies on the properties of starch-based edible films and coatings has been discussed in this review. Overall, the review presents state-of-the-art information about important properties pertaining to starch-based edible films and coatings, including rheological, thermal, mechanical, microstructural, and barrier properties.

Received 6th November 2023
Accepted 25th January 2024

DOI: 10.1039/d3fb00211j

rsc.li/susfoodtech

Sustainability spotlight

'Plastification' of the planet has emerged as the biggest environmental challenge that includes greenhouse gas emissions, microplastic pollution, and the imbalance of ecosystems, and it has led to increased attention to sustainable packaging. The thrust of current research is to develop a wide range of biodegradable packaging and edible films (EFs) to counter conventional packaging. Various sources, including marine-based, agro-based, and valorized materials, have been used to fabricate sustainable packaging materials. The inherent properties of edible films remain the bottleneck for their implementation, and therefore, property improvement remains the essential key for replacing conventional plastics with EFs in the food industry. EFs are basically a thin layer of biopolymer coating containing polysaccharides and proteins on the food surfaces so that they can be consumed directly with the food. The interest in such edible films and coatings has increased significantly in recent years. Among a variety of resources, starch has been used for the formation of films and coatings with a range of properties. Similar to other biopolymers, starch has limitations in its desired film properties for industrial applications. To impart the desired properties, many approaches have been employed, including starch modification, incorporation of low-molecular-weight plasticizers, blending of polymers, and reinforcement of active ingredients and nanoparticles. The property improvement is quite promising; however, more attention is necessary so that edible starch-based packaging could increase the market share of EFs in the packaging industry. The present review summarizes systematic progress in starch-based edible films, their blends, and coatings incorporated with bioactive compounds and nanoparticles. Additionally, the challenges and opportunities in starch-based edible packaging have been discussed.

1. Introduction

Conventional polymers have been used for centuries as a material for food packaging. Plastic pollution is everywhere, on land, in lakes, rivers, and beaches, and even in extreme remote locations, including the Arctic and Antarctic, with increasing plastic use and its accumulation negatively affecting the global environment and human beings. Additionally, plastic is one of the major sources of greenhouse gas emissions. These factors are the driving forces behind the development of and focus on sustainable packaging.[1] Researchers are continually making efforts to develop various types of biodegradable packaging and edible films (*e.g.*, marine-based, agro-based, and valorized materials) with limited success.[2] Very few of these have been commercialized. The bottleneck for biodegradable edible films (EF) is their inherent properties, which are not yet comparable with those of conventional polymeric films. Therefore, property improvement is essential to replace conventional plastics with EFs in the food industry.[3]

[a]*Food & Nutrition Program, Environment and Life Sciences Research Center, Kuwait Institute for Scientific Research, P.O. Box 24885, Safat, 13109, Kuwait. E-mail: jahmed2k@yahoo.com; jaahmed@kisr.edu.kw*

[b]*Department of Food Process Engineering, National Institute of Technology Rourkela, India*

EFs are essentially a thin layer of biopolymer coating on the surfaces of food materials that can be consumed directly with the food. An EF acts as a barrier on the food surface, permitting selective exchange of gases (*e.g.*, carbon dioxide and oxygen), limiting mass transfer (*e.g.*, moisture and solute migration), and slowing the oxidative reaction rate.[3] The EF is prepared using biopolymers, namely, polysaccharides and proteins, which are edible, biodegradable, non-toxic, and biocompatible.[4] The interest in such edible films and coatings has increased significantly in the last few years. Recent data indicated a tremendous increase in the number of publications on edible films, in particular from 2020 to 2022, which occupied about 50% of the total publications in the last decade (2012–22).[5]

Among a variety of resources, starch is abundant in nature and has the potential for conversion into biodegradable edible packaging.[6] Various studies have been reported on the usage of starch from a range of sources for the formation of films and coatings with a variety of properties.[7]

Starch lacks the desired film properties, in particular barrier, thermal, and mechanical properties, for its industrial applications when compared with other polymers.[8] To impart the anticipated properties to starch, various approaches have been implemented, including modification of starch,[9,10] plasticization using various low molecular weight plasticizers,[11–13] eutectic solvents,[14] blending of polymers,[15–18] reinforcement of active ingredients such as essential oils,[19–21] natural extracts,[22,23] and nanoparticles (*e.g.*, quantum dots,[14] cellulose, ceramics,[13] metals and metal oxides[24]). The property improvement approaches were quite successful; however, more attention is required so that edible starch-based packaging could increase the market share of EFs in the packaging industry.

So far, no review work has emphasized the impact of various strategies on the mechanical, thermal, rheological, barrier, and microstructural properties of edible starch-based packaging. To fill the gap, this review has focused on recent progress in the properties of starch-based edible films, their blends, and coatings incorporated with bioactive compounds and nanoparticles. Additionally, we have also covered the recent patents on starch-based edible packaging materials. Finally, the challenges and opportunities of starch-based edible packaging applications are discussed. Several internet databases (*e.g.*, Science Direct, Wiley Online Library, ACS Publication, and open-access journals) were searched to obtain the appropriate papers related to the topic and contents. This review contains most of the articles published from 2019 to July 2023.

2. Key properties of starch-based edible coatings and films

There are several key properties for the development and functions of edible films (EFs) and coatings, which include mechanical, rheological, thermal, microstructural, and barrier properties. The properties of starch-based EFs and coatings mostly depend on the characteristics and type of starch used.[25] The properties of starch may vary based on the source, such as cassava, potato, corn, maize, tapioca, rice, sago, wheat, banana, quinoa, barley, mung beans, peas, oats, and taro.[26] Naturally, films made from various starch formulations would have distinct properties.[27] For example, different types of starch result in films with different thicknesses, which can affect various properties of films such as mechanical and barrier (against water vapor, light, and oxygen) properties.[26] Regarding this, the same concentration of starch from different sources, namely potato, corn, and wheat, formed films with varying thicknesses of 0.227 mm, 0.196 mm, and 0.189 mm, respectively.[26] There are many other properties of starch that can affect the characteristics of films, such as amylose/amylopectin content and the size and shape of granules.[28] Apart from the type of starch, processing parameters (time and temperature), storage conditions, and different additives can highly influence the properties of starch-based edible films.[21]

Mechanical properties such as tensile strength (TS), elongation at break (EAB), and Young's modulus (YM) provide the flexibility and strength of edible films.[26] When choosing a film-forming material, it is important to preserve the integrity of food during storage, handling, and distribution.[29] In addition, water vapor permeability (WVP) is another important property of edible films that restricts water vapor transfer in packaged food products.[26] The water vapor may transfer from the internal or external environment through the packaging film, which may result in a reduction in food shelf-life and its deterioration.[30,31] Furthermore, the morphological properties show the smoothness/roughness, compactness, cracks, and holes on the surface of packaging films. These may affect other properties such as surface hydrophobicity, WVP, and mechanical, and optical properties.[32] Similarly, the XRD pattern presents the crystalline and amorphous nature of edible films. Most edible films have a semicrystalline nature to maintain their integrity, strength, and flexibility[33] The rheological properties of the film determine the process of film formation and its casting. They also demonstrate the impact of force, temperature, and time on the viscoelastic behavior of packaging films or coatings, which is very important during handling, distribution, and storage.[34,35] The thermal analysis of the films reveals the thermal stability and phase transition of edible films when exposed to different temperatures.[32] In this review, a brief discussion about each parameter of edible films and coatings has been elucidated. The effects of additives in starch-based edible films and coatings and their characteristics have also been discussed.

3. Rheological properties of starch-based filmogenic solutions

Rheology measures the flow and behavior of liquid and semi-solid foods. Similar to other materials, the rheology of starch-based filmogenic solutions can be investigated over a wide range of frequencies, shear rates, temperatures, or times. Both steady-state flow and oscillatory shear (SAOS) can be used for rheological measurements. The casting ability of filmogenic solution can be predicted by its surface smoothness at low shear viscosity. A thick consistency or a high magnitude of apparent viscosity in the film solution is not desired because removing

the entrapped film layer is too difficult in these cases. Among rheological parameters, the most important are the apparent viscosity (η), flow behavior index (n), consistency index (K), yield stress (τ_0), elastic (G') and viscous modulus (G''), and complex viscosity (η^*). These parameters can be correlated with filmogenic solutions to obtain a high correlation with the smoothness of the edible films. A brief review of the rheological properties of film-forming solutions that led to the development of starch-based edible packaging is presented in this section. Steady flow and oscillatory rheology are discussed separately to make it easy for the readers.

3.1 Steady flow behavior of filmogenic solutions

The flow properties of FFS can be characterized by using some conventional rheological models. The model parameters can be compared and used for process optimization. The most frequently used flow models are the power law and Herschel–Bulkley models (eqn (1)), where shear stress (τ) and shear rate ($\dot{\gamma}$) are plotted against each other. The latter one is applied to a fluid under yield stress (τ_0).

$$\tau = \tau_0 + K\dot{\gamma}^n \quad (1)$$

where K refers to the consistency index (Pa s^{-1} n) and n refers to the flow behavior index (dimensionless). Eqn (1) converts to a power law model for fluids without yield stress.

Simultaneously, plotting the apparent viscosity against the shear rate yields many rheological models. The readers can read about those models elsewhere.[35] Only specific models are included in this review.

The flow rheology of FFS containing tapioca starch, glycerol, and decolorized hsian-tsao leaf gum (dHG) was investigated.[36] The FFS was prepared following sequential heating and cooling steps (heating to 95 °C/hold for 30 min; cooling to room temperature/hold for 50 min). The steady-shear rheology of FFS indicated a typical structured material which exhibited a Newtonian behavior at low shear rates and a shear-thinning behavior at higher shear rates due to the entanglement structure, which could not be restored immediately. The steady-shear data fitted the modified Carreau model (eqn (2)) well by ignoring the infinite shear viscosity.

$$\eta = \eta_0[1 + (K_1\dot{\gamma})^2]^{(n-1)/2} \quad (2)$$

where η is the apparent viscosity (Pa s), $\dot{\gamma}$ refers to the shear rate (s^{-1}), η_0 is the limiting viscosity at a low shear rate, K_1 is a characteristic time constant which is related to the relaxation time of the polymer in solution, and n refers to the power-law index. The results showed that η_0 of starch/dHG FFS increased overall, and n decreased with an increase in the concentration of dHG. These data suggest the formation of a new structure through entanglement formation and interactions between starch and dHG. Glycerol has a minimal effect on steady shear viscosity. Similarly, the steady-state flow rheology of corn starch (CS)/methylcellulose (MC)/glycerol (GR) blend filmogenic solutions exhibited shear-thinning behavior.[37] Shear stress–shear rate data competently fitted the Herschel–Bulkley

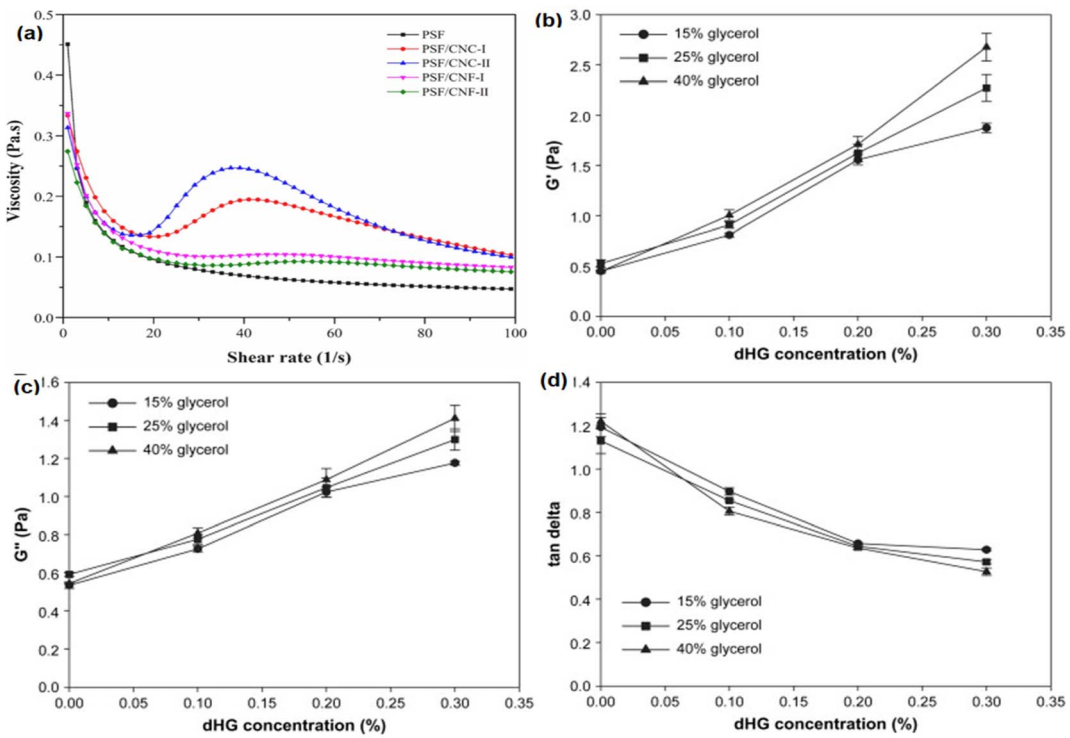

Fig. 1 (a) Steady-state flow behavior of cellulose nanoparticle-loaded pumpkin starch-based FFSs and[39] (b) storage modulus, (c) loss modulus, and (d) tan δ behavior of dHG and glycerol incorporated tapioca starch-based FFSs.[36]

model. The flow behavior index (n) of the filmogenic solution ranged from 0.37 to 0.90, indicating the shear-thinning behavior of the fluid. The FFS showed a positive yield of 38 mPa for the formulations without MC, and the yield value increased to 433 mPa when 62% MC was incorporated.

Shear-thinning behavior is reported for the modified starch and nanoemulsion-based starch film-forming solutions. Cross-linked faba bean starch with sodium trimetaphosphate (STMP) (1–5%) showed shear-thinning behavior.[38] The STMP cross-linking restricts the intermolecular polymer–polymer chain bonding, which results in a drop in the yield stress and consistency index of the starch pastes. Similarly, the FFS containing pumpkin starch, cellulose nanocrystals (CNCs), and cellulose nanofibers (CNFs) produces shear-thinning fluid.[39] The FFS of pumpkin starch, however, suddenly transformed into a shear thickening behavior at a shear rate of 23 s^{-1} with the addition of CNCs and CNFs (Fig. 1a). The pumpkin starch FFSs loaded with CNCs showed distinct shear thickening behavior compared to CNF-based FFSs, attributed to the higher contact area of CNCs that facilitates strong network formation and increases viscosity. Furthermore, all the blended filmogenic solutions had a low shear viscosity, which was suitable for the casting of films.

The flow rheology of edible filmogenic solutions prepared with native (NPS) or octenyl succinylated potato starches (OSAS) and honey-bee extracts (HBE) displayed improvement.[40] Shear stress–shear rate data from FFS adequately fitted the power law model. The esterification process and the loading of HBE into the NPS improved the K values significantly, from 9.40 to 311.69 Pa s^n of the starch. On the other hand, the esterification process decreases the n values of starch pastes, which further drop upon the incorporation of HBE into the NPS. The flow index for native and OSA starch pastes remained below unity, suggesting that the pastes were pseudoplastic fluids. A separate study reported that the flow properties of cassava starch/chitosan blend films weakened when pitanga leaf extract and natamycin were incorporated into the blend.[41] The η and K of the control FFS decreased from 95 to 75 mPa s and 0.44 to 0.30 Pa s^n, respectively, indicating structural weakening and less compact interactions between extracts and polymers.

3.2 Oscillatory rheology of filmogenic solutions

The mechanical spectra of filmogenic solutions during oscillatory measurements are frequency dependent. In a lower frequency range, the CS/MC/GR solutions exhibited liquid-like ($G'' > G'$) behavior, which transformed into solid-like behavior ($G' > G''$) in the higher frequency range with higher MC contents.[37] The development of network formation occurred on a longer time scale (low frequency) because of the entanglement of polymer chains, and at high frequencies, there was not enough time for the inter-chain entanglements and the resultant solution to produce a gel structure. The CS/MC/GR filmogenic solutions followed the Cox–Merz superposition principle (eqn (3)), while the apparent viscosity from the steady flow was plotted against the complex viscosity of oscillatory rheology in an equal frequency range and at an equal shear rate. The fit of the rule supports the topological entanglement interactions of individual species. Among the constituents, MC showed the highest influence on the rheological properties of corn starch-based film-forming dispersions.

$$|\eta(\dot{\gamma}) = \eta^*(\dot{\gamma})|_{\omega=\dot{\gamma}} \quad (3)$$

where τ_0 is the yield stress and $\eta(\dot{\gamma})$ and $\eta^*(\dot{\gamma})$ are shear and complex viscosities, respectively.

Another work reported that FFS of tapioca starch, dHG, and glycerol had a predominant solid-like behavior ($G' > G''$), which was completely different from that of the FFS made from starch-alone solutions (liquid-like behavior) (Fig. 1b–d).[36] This indicates network formation among constituents during heating and cooling of the solutions. Moreover, the increase in glycerol concentration (15 to 40%) gradually increased the storage modulus (G') and the loss modulus (G'') of the FFSs and decreased the tan δ values.

An edible film was formulated by blending starch (an equal weight mixture of native rice starch and hydroxypropyl cassava starch), maltodextrin (0–60% w/w), agar (0–30% w/w), and glycerol (as a plasticizer) and assessing their film-forming solution rheology by oscillatory temperature sweep measurements from 50 to 95 °C at 1 Hz.[15] The G' of the solutions increased abruptly at around 57 °C and dropped immediately, indicating gelatinization, where swelling and breakdown of starch crystallites occurred. The blend with increased agar concentrations exhibited the highest G' because of the decreased availability of water and increased polymer mixtures. The blend with the least amount of starch attained the maximum phase angle (δ) of 22°, exhibiting a low solid-like behavior that decreased significantly on increasing the agar content. An introduction of new polysaccharides other than starch has restricted the number of junction zones and makes the blend constituents thermodynamically incompatible, increasing mechanical rigidity. Overall, the oscillatory rheology of starch-based edible films and coatings provides important information about film formation, processibility, and mechanical strength. It also demonstrates the impact of force, temperature, and time on the viscoelastic behavior of packaging films or coatings, which plays an important role in handling, distributing, and storing food products.[34,35]

4. Scanning electron microscopy (SEM)

The microstructure is crucial for controlling the mechanical and barrier properties of edible films and coatings. Understanding the microstructure and the interaction of film ingredients is significant, both for the basics of materials science and from a practical point of view. Among structural measurement tools, scanning electron microscopy (SEM) is used to examine the miscibility of components, smoothness, defects, and performance of the film.

Micrographs of plasticized corn starch films produced by extrusion and casting displayed irregular surface structures.[42] Additionally, it was observed that starch microstructures

remained unaffected in the extrusion process, which might be due to partial gelatinization of the film blend. Micrographs of the cast films showed that corn starch remained in its native state in agglomerates, which could be attributed to the presence of plasticizers in the matrix. In a separate study on pregelatinized corn starch-based edible films, it was reported that the addition of cellulose nanofibers (CNFs) and basil essential oil (BEO) increased the surface roughness of the films.[43]

The extent of miscibility and compatibility of starch with other polysaccharides (*e.g.*, agar and maltodextrin) in the film matrix demonstrated that maltodextrin produced a smooth surface, whereas the agar introduction led to the aggregation of fine clumps with a rough surface.[15] Moreover, the addition of maltodextrin led to wrinkled structures due to its high water-absorbing capacity. The absorbed water evaporates during drying, and shriveled networks lead to wrinkled structures. Therefore, the results demonstrate that the limited agar concentration leads to strong gels with rigid networks in the starch matrix. The microstructure of edible bilayer films [corn/wheat (CW) and zein (Z) starch] is controlled by using the structural architecture of components in the dispersion.[44] SEM micrographs showed that the film made with only CW starch had a non-homogenous surface with insoluble starch granules and a thinner and more intensive cross-section. The blend film containing the lowest amount of zein had a smooth surface with a highly compacted cross-section. A SEM micrograph of the starch and gelatin blend film displayed smooth surface morphology, indicating good molecular compatibility between starch and gelatin.[45] Furthermore, adding resveratrol at lower concentrations (10%) to the potato starch/gelatin blend film did not significantly affect the surface morphology of the films. However, resveratrol particles were observed on the surface at 20% concentration, suggesting the agglomeration of resveratrol particles, making them rough. Blended edible films (AS/IC) from arrowroot starch (AS) (2 to 3.5%) and iota-carrageenan (IC) (0.5 to 2%) were prepared and compared against AS (4%) films.[46] SEM micrographs of the AS (control) films had a smooth and homogenous surface. However, increasing IC contents resulted in irregular and rough surfaces on the AS/IC samples, indicating high matrix chain interactions among polymers. Moreover, irregular surface structures correlate with high opacity values in the composite films, whereas smooth and uniform surfaces correlate with low opacity. Similarly, the morphology of the films based on pearl millet starch (PMS) had a smooth surface over a blend of composite films of PMS and carrageenan gum, where the film showed a rough, coarse, and partially irregular surface.[33] Similar microstructures were also observed for the *k*-carrageenan and Proso millet starch films.[47]

In another study, potato starch and chitosan blend films had smooth and compact surface structures, revealing the compatibility of polymers.[48] The addition of citric acid (CA) as a cross-linker significantly affected the morphology of composite films. The CA cross-linked films demonstrated a coarse-textured surface, possibly due to the solidified CA crystals on the surface at a higher concentration (20%). In addition, the 3-D surface topographic images confirmed the increased roughness with increasing CA concentration in potato starch/chitosan composite films. Similarly, the pumpkin starch film exhibited a smooth and uniform microstructure, attributed to the appropriate starch gelatinization and glycerol plasticization processes.[39] In addition, the incorporation of CNCs and CNFs did not affect the homogenous surface of the nanocomposite films, indicating the compatibility between nanocellulose and starch. A similar study was also reported, where the incorporation of banana peel nanocellulose fibers (BPNCFs) did not alter the smooth surface morphology of the banana peel starch-based edible film.[49] On the other hand, the incorporation of cellulose nanocrystals (CNCs) in the arrowroot starch/carnauba wax nanoemulsion films led to roughness, attributed to the aggregates of CNCs.

An edible film from cassava starch and cinnamon essential oil (CEO) was developed.[20] Micrographs demonstrated that the film prepared without CEO had an uneven surface without any pores or cracks, and the structure was vesicle-like. However, the CEO plasticized films exhibited a coarse surface with cracks, wrinkles, and holes. Such defects on the film surface could be developed due to flocculation, coalescence, high volatility, and emulsification of CEO during the drying process. The micrograph of the cross-section displayed a uniform distribution of CEO without any delamination, and pores in the matrix were attributed to the appropriate emulsification effect of the surfactant. A similar observation was reported, where they prepared films from chayote tuber starch (CTS) incorporated with zein–pectin nanoparticle-stabilized cinnamon essential oil Pickering emulsion (ZPCO) at selected concentrations.[50] It was observed that the addition of ZPCO at 4% w/w resulted in the development of micropores because of the evaporation of essential oil and produced a rough surface on the CTS film.

Micrographs of composite films prepared from potato starch/Zedo gum/*Salvia officinalis* essential oil (EO) revealed that the reinforcement of EO improved the smoothness and reduced the gaps and cracks on the surface of the film.[51] The smoothness could be due to the hydrophobic and greasy characteristics of oil, which cross-links the structure to cover the surface and seal the gaps. Conversely, incorporating *Mentha spicata* and *Cymbopogon martinii* EOs into arrowroot starch/carnauba wax nanoemulsion/cellulose nanocrystal films led to heterogeneous surfaces.[52] Increasing the concentration of EOs from 0.1 to 0.3% resulted in holes on the surface of the films (Fig. 2a–d). Additionally, at a higher concentration, the oil droplets affect the immobilization of the emulsion within the film matrix. The incorporation of phenolic compounds can significantly affect the surface morphology of starch-based edible films. Chen and his group[61] reported that the addition of phenolic compounds such as protocatechuic acid (PA), naringin acid (NA), and tannic acid (TA) in the maize starch/carboxymethylcellulose/konjac glucomannan blend film (MS/CMC/KG) increased the surface roughness. A separate study found that adding broccoli leaf polyphenols (BLPs) to a tapioca starch/pectin (TSP)-based film yielded a higher density structure than that of the control TSP edible film. This observation suggested that BLPs played an important role in promoting the cross-linking bonds between pectin and tapioca starch.[54]

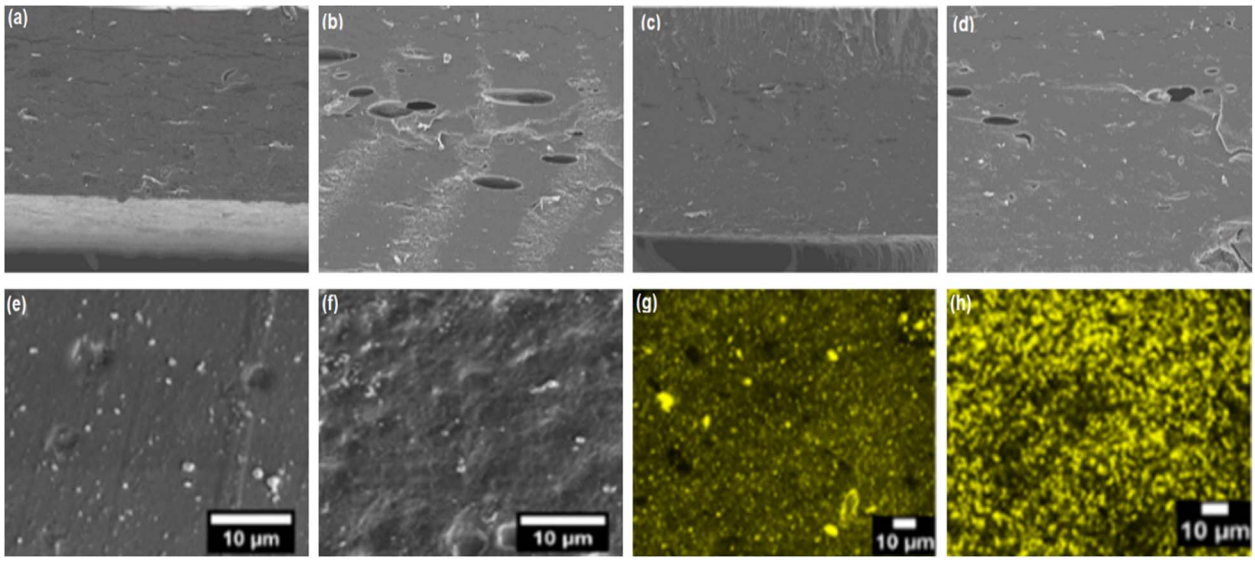

Fig. 2 Micrographs of edible films (a) arrowroot/carnauba wax nanoemulsion/cellulose nanocrystals/*Mentha spicata* essential oil (0.1%), (b) arrowroot/carnauba wax nanoemulsion/cellulose nanocrystals/*Mentha spicata* essential oil (0.3%), (c) arrowroot/carnauba wax nanoemulsion/cellulose nanocrystals/*Cymbopogon martini* essential oil (0.1%), (d) arrowroot/carnauba wax nanoemulsion/cellulose nanocrystals/*Cymbopogon martini* essential oil (0.3%),[52] (e) sago starch/guar gum/carvacrol (0.75%), and (f) sago starch/guar gum/carvacrol (0.75%)/citral (1.0%). Confocal laser scanning microscopy of (g) sago starch/guar gum/carvacrol (0.75%) and (h) sago starch/guar gum/carvacrol (0.75%)/citral (1.0%).[19]

The addition of carvacrol and citral EOs to the sago starch/guar gum-blend film led to irregularities in the film surface (Fig. 2f).[19] The citral-loaded sago starch/guar gum films had less roughness than the carvacrol-loaded films at a similar concentration (0.75%) (Fig. 2e). The roughness in the film structure occurred due to the layer formation, and the blending restricted the evaporation of solvent from the surface of the film, resulting in the pores. Confocal microscopy of both EO incorporated sago starch/guar gum films demonstrated the homogeneous dispersion of spherical oil droplets compared to that of films produced with a single EO (Fig. 2g and h). The amalgamation of citral droplets was, however, observed with cluster formation. Similarly, the incorporation of CEO resulted in a rough surface with wrinkles, cracks, and pores from cassava starch films.[20] The incorporation of oregano essential oil (OEO) in *Dioscorea zingiberensis* C. H. Wright's (DZW) starch film demonstrated a surface morphology with wrinkles and micropores.[55] The reason for such discontinuities in the EO-loaded starch films could be the volatility, coalescence, flocculation, and emulsification of EO during drying, which affect the resultant film properties.

The incorporation of epigallocatechin (EGCG), blueberry ash (BBA), and macadamia skin (MAC) extracts at a lower concentration into the pea starch/guar gum blend film led to a homogeneous, soft, and intact surface.[16] SEM micrographs became rough and bumpy at a higher concentration of extracts, which might be because of the higher number of interactions between the polymer and polyphenol compounds. Microscopic imaging by the Nomarski DIC technique on the corn starch (CS)/methylcellulose (MC)/fireweed extract (FE; 0.0125–0.05% w/w) edible films demonstrated the presence of numerous hydrothermally disrupted starch granules in the FFS of CS.[23] The starch granules completely lost their internal crystalline structures, as confirmed by the absence of Maltese crosses under polarized light. The SEM micrographs of the dried CS-based

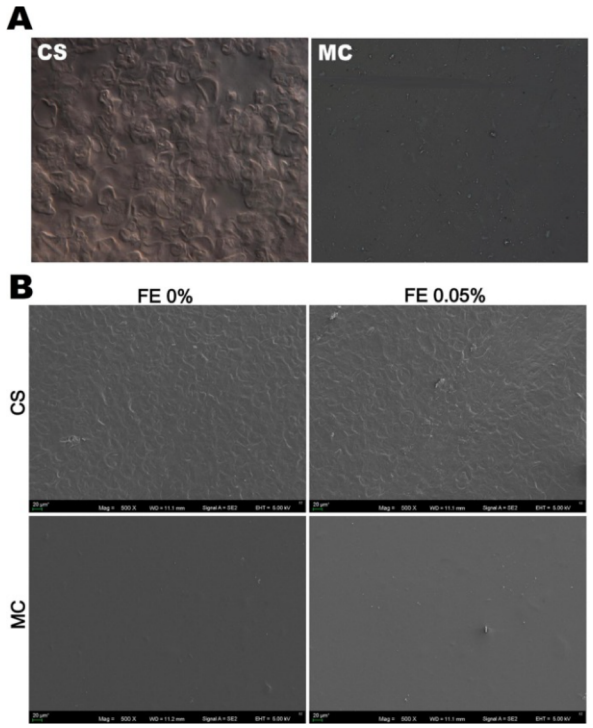

Fig. 3 Morphology of the control film-forming solutions (at 400× magnification) based on corn starch (CS) and methylcellulose (MC) examined using Nomarski DIC microscopy (A). Micro-topographies of films based on CS and MC without and with fireweed extract (FE) (B).[23]

films showed rough surfaces. On the other hand, the MC-based films showed a smooth topography, as observed through light microscopy (Fig. 3). The authors concluded that gelatinization has a significant effect on the film formation solution and ultimately the film. They found that cooked CS produced a film with higher transparency than the film made from the FFS that underwent a thermal treatment at 90 °C, where gelatinization remained incomplete.

5. Atomic force microscopy (AFM)

AFM of the starch-based films provides valuable information on the surface morphology and the developed surface roughness of the films. The surface of corn–wheat starch (CW) films without the addition of zein had the most bulges (Fig. 4a2).[44] The bilayer Z/CW-based edible films with selected zein contents had relatively continuous and smooth matrices with fewer cracks and pores (Fig. 4b1, b2, c1, and c2). The surface roughness of the film increased on increasing the concentration of zein (Fig. 4d1, d2, e1, and e2). Moderate incorporation of zein increased the film surface smoothness; however, it is not economically feasible. The arithmetic mean (S_a) and root mean square (S_q) values of the film can affect its physical and mechanical properties. An addition of 0.06 g of zein to CW films resulted in the lowest surface roughness, and a higher concentration of zein assisted in creating a rough surface on the film.

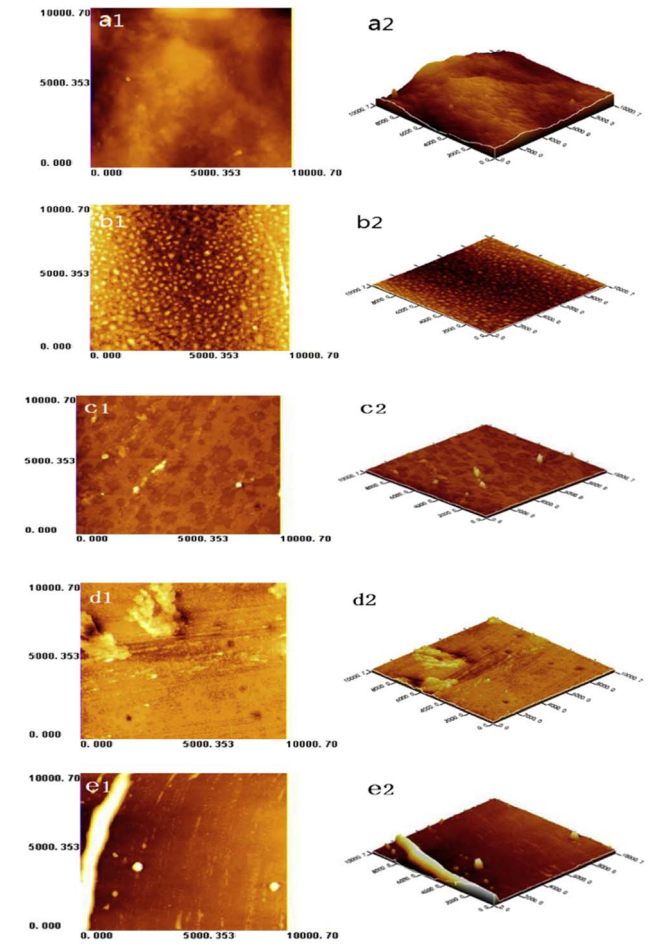

Fig. 4 Typical AFM images and S_a and S_q of the corn/wheat starch and zein bilayer films. (a1) and (a2) showed CW10/Z0; (b1) and (b2) showed CW10/Z1; (c1) and (c2) showed CW10/Z2; (d1) and (d2) showed CW10/Z3; (e1) and (e2) showed CW8/Z3. (a1), (b1), (c1), (d1) and (e1) showed a two-dimensional structure of AFM images, (a2), (b2), (c2), (d2) and (e2) showed a three-dimensional structure of AFM images.[44]

The topography of plasticized corn films, which were produced in two stages (extrusion followed by casting), displayed a heterogeneous and rough surface.[42] It is reasoned that the gelatinization of corn starch was incomplete in the casting technique, keeping residues of starch granules (*e.g.*, amylopectin) that played a major role in the development of a rough surface. The three-dimensional topography of the film showed some smooth regions on the surface and ripples with different heights ranging from 50 to 300 nm. The smooth regions are believed to be attributed to plasticizers, and the ripples represent the presence of extra granular amylopectin on the surface of the film.

The addition of extra virgin olive oil (EVOO) to the palm starch/chitosan blend film led to a reduction in surface roughness.[56] It has been observed that the smoothness of the film is directly related to the concentration of EVOO, both qualitatively and quantitatively. The S_a and S_q of the EO-blended films were reduced significantly from 305 to 89 nm and 400 to 112 nm with 5% EVOO (w/w), respectively. Similarly, adding apple peel polyphenols reduced the roughness from 52.3 to 16 μm in the cassava starch/carboxymethylcellulose films.[22] For the banana peel starch-based edible film, the roughness parameters S_a and S_q were 9 and 14.08 μm, respectively.[49]

6. Fourier transform infrared spectroscopy (FTIR)

FTIR is a rapid, non-destructive molecular characterization technique of materials' structural architecture and configuration, and the interplay of functional groups. FTIR is routinely used in food packaging to establish interactions among constituents or the disappearance of some bands during processing. The molecular interactions of starch, agar, and maltodextrin in the film system were characterized by FTIR.[15] The starch films exhibited a sharp peak at around 1300 to 1000 cm^{-1}, characteristic of $-CH_2$ bending, and C–C, C–O, O–H, and C–O–H stretching vibrations. The agar addition reduced the intensity of these stretching vibrations, attributed to the modified amorphous and helical structure conformations of starch molecules in the blend films. On the other hand, maltodextrin acts as a filler in the starch–agar matrix by increasing the intensity of these peaks. However, both agar and maltodextrin reduced the intensity of the broad absorption peak between 3700 and 3000 cm^{-1}, which correlates with the free, inter, and intra-molecular hydroxyl groups in the film matrix. The available hydroxyl groups were reduced in the blend films due to the binding of free water with hydroxyl groups in maltodextrin and agar.

FTIR spectra of an optimized pearl millet starch (PMS)/carrageenan (CG)-based film, PMS, and CG films were

compared to understand the interactions among constituents.[33] The bands detected at 3272 cm^{-1}, 3280 cm^{-1}, and 3250 cm^{-1} characterized the stretching frequency of the OH– group in neat PMS films, PMS/CG films, and CG films, respectively. The addition of CG resulted in a shift in the OH– and C–H absorption bands to higher wavenumbers, confirming the blending of components in the composite films. Additionally, the formation of a different peak at 1727 cm^{-1} in the PMS/CG composite films indicates a higher degree of cross-linking between the polymers. Similarly, the addition of iota-carrageenan shifted the O–H stretching bands to higher wavenumbers in the blended films of arrowroot starch.[57] In addition, the intensity of the amide peak at 1635–1646 cm^{-1} decreased, and that of the COO– stretching vibration peak (1583–1587 cm^{-1}) of carrageenan increased in the blend films.

The FTIR spectra of cross-linked MBS films influenced by citric acid concentrations are illustrated in Fig. 5.[58] It can be seen that the untreated starch films exhibited characteristic peaks of polysaccharides at wavenumbers of 858 cm^{-1} and 926 cm^{-1} (C–H bending), 999 cm^{-1}, 1077 cm^{-1}, and 1150 cm^{-1} (C–O stretching), 1340 cm^{-1} (C–O–H bending), 2929 cm^{-1} (aliphatic C–H stretching), and 1644 cm^{-1} and 3288 cm^{-1} (O–H stretching). With CA cross-linking, a new peak showed up at 1721 cm^{-1}, and the intensity of this peak increased with increasing concentrations of CA. The observed peak is assigned to the C=O stretching vibration, which indicates the esterification reaction between starch and CA. Similarly, the appearance of a new peak at 1724 cm^{-1} was observed in the CA cross-linked potato starch/chitosan blend films.[48] The intensity of the characteristic broad peak at 3285 cm^{-1} decreased with the increase in CA concentration up to 15%, ascribed to the cross-linking reaction between polymers and CA, which reduced the free O–H groups in the films. The reduction of available O–H groups in the CA cross-linked tapioca starch films was also correlated with the ratio of peak intensities at 3300 and 1149 cm^{-1}.[59]

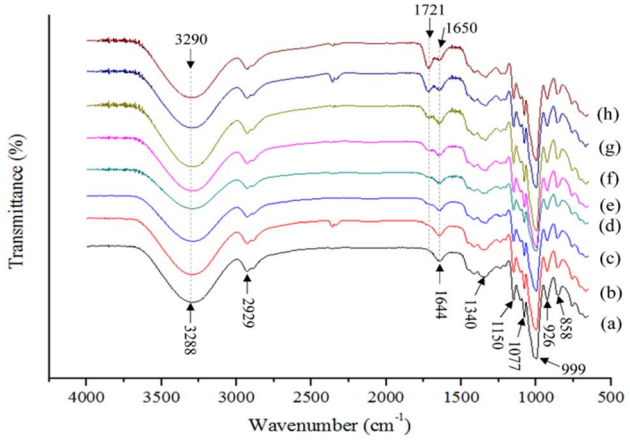

Fig. 5 FTIR-ATR spectra of edible films made of mung bean starch (MBS) cross-linked with citric acid (CA). (a) MBS-0-CA, (b) MBS-1-CA, (c) MBS-2-CA, (d) MBS-3-CA, (e) MBS-4-CA, (f) MBS-5-CA, (g) MBS-10-CA, and (h) MBS-15-CA.[58]

The EO-loaded starch films showed distinct changes in the FTIR spectra. The incorporation of CEO in the cassava starch matrix demonstrated significant sharp peaks at 2926, 1678, and 1127 cm^{-1}, which are characteristic of C–H, C=O, and C–O–H stretching of CEO, respectively.[20] In addition, new absorption peaks appeared at 752, 691, and 1454 cm^{-1} attributed to the phenyl group of incorporated cinnamaldehyde in films. Moreover, the broad absorption peak at 3398 cm^{-1} in the starch film shifted to a lower wavenumber with reduced intensity, indicating the hydrogen bonding interactions between CEO and starch. Similarly, adding *Salvia officinalis* essential oil changed the potato starch spectrum completely, wherein new peaks appeared in the region of 500–1500 cm^{-1}, indicating the interaction of the polysaccharide matrix and fatty acids (hydrocarbons) from essential oil.[51] The addition of the zein–pectin nanoparticle-stabilized cinnamon essential oil-based Pickering emulsion (ZPCO) in the chayote tuber starch (CTS)-based film significantly reduced the peak intensity in the range of 3000 to 3500 cm^{-1} and wavenumber 2927 cm^{-1} suggesting the reduction of O–H bond stretching in the film matrix. In addition, the characteristic peaks at 1122 cm^{-1}, 1624 cm^{-1}, and 1668 cm^{-1} in ZPCO-added CTS films indicated the presence of cinnamaldehyde and other phenolic compounds.[50] Similarly, the addition of oregano EO in the starch-based film significantly diminished the peak intensity between 3100 and 3600 cm^{-1} (associated with O–H bond stretching of the hydroxyl group and water molecules), suggesting the interaction between phenolic compounds and starch molecules.[55]

The pea starch/guar gum blend film showed some changes in the FTIR spectrum because of the incorporation of natural extracts [blueberry ash fruit extract (BBA), epigallocatechin gallate (EGCG), and macadamia peel extract (MAC)].[16] The broad peaks in the 3000 to 3600 cm^{-1} range became wider and sharper in the extract-loaded films, suggesting that the O–H and C=H bonds of polyphenols undergo intermolecular interactions with polymers. Additionally, the peaks between 1500 and 1675 cm^{-1} (stretching vibration of CO and bending vibration of C–O–H bonds) became more evident due to inter and intramolecular cross-linking of O–H and CO after the addition of a natural extract to the PSGG film. The potato starch films exhibited characteristic peaks at 3293 and 2924 cm^{-1}, assigned to intermolecular or intramolecular –OH and C–H stretching. The potato starch films incorporated with purple corn cob extract (anthocyanin) showed a higher peak intensity at 1648 cm^{-1} than the neat potato starch film, suggesting the immobilization of anthocyanin in the starch film matrix. The characteristic peaks at 924 and 1150 cm^{-1} represented the C–O stretching bond. However, the addition of mole essential oil (MEO) led to a variation in the peak intensity at 3293 cm^{-1}, suggesting an interaction between the –OH groups of MEO and potato starch.[60]

The FTIR spectra of the banana peel starch-based edible film showed higher intensity at 1022 cm^{-1}, suggesting the gelatinization of starch during the film preparation. On the other hand, the intensity of the peak at 1022 cm^{-1} further increased after the addition of banana peel nanocellulose fibers (BPNCFs) representing the glycosidic linkage, which may be due to the

interaction between BPNCFs and banana peel starch molecules.[49,61] Edible corn starch (CS)-based films incorporating nanofibrillated cellulose (NFC) and nanofibrillated lignocellulose (NFLC) were developed separately with different concentrations of NFC and NFLC. In the chemical interaction study, they found that the O–H stretching (peak at 3283 cm^{-1}) and C–O bending (peak at 1652 cm^{-1}) vibrations observed in the CS film shifted toward a higher wavenumber after the incorporation of NFC and NFCL individually. This shift in the peak suggested an interaction between starch and cellulose molecules.

The chemical interactions among starch, other biopolymers, and chemicals can be observed through spectral changes, including peak shift and broadening in FITR spectra. For starch/gelatin/resveratrol-based composite films, the addition of gelatin to starch demonstrated the formation of strong hydrogen bonding that increased the intensity at 3280 cm^{-1}. The addition of resveratrol in the potato starch/gelatin composite film led to a characteristic peak of benzene ring vibration (at 1510 cm^{-1}), confirming the presence of phenolic compounds. The addition of resveratrol (20% w/w) in the potato starch/gelatin film further increased the intensity of the peak at 1630 cm^{-1} and shifted the band position from 3280 cm^{-1} to 3269 cm^{-1}, suggesting the influence of resveratrol on the polymer matrix by reinforcing the hydrogen bonds.[45] The composite film based on tapioca starch, pectin, and broccoli leaf polyphenols (BLPs) showed major absorbance peaks at 3300 cm^{-1} (O–H stretching vibrations), 2900 cm^{-1} (C–H stretching vibrations), 1735 cm^{-1} (C=O stretching vibrations), 1607 cm^{-1} (C=C vibrations), 1228 cm^{-1} (C–O bond stretching), and 1011 cm^{-1} (C–O–C stretching vibrations). The addition of BLPs to the TSP film did not lead to any significant difference in the FTIR spectra of the film. However, on the addition of BLPs at a higher concentration (3%), the peak at 3276 cm^{-1} associated with O–H stretching vibrations of the TSP film without BLPs shifted to 3281 cm^{-1}. This shift of the peak to a higher wavenumber suggested the increase in the hydrogen bonding between tapioca starch and pectin due to BLPs.[54]

7. X-ray diffraction (XRD)

XRD is extensively used to characterize the material properties of films, including crystals, dispersion of fillers in composite films, and other surface properties. Starch is a semi-crystalline biopolymer containing both crystalline and amorphous phases contributed by amylose and amylopectin. During film formation, the crystalline peaks of the starch molecules are transformed into semi-crystalline or amorphous patterns due to granular disruption, and the dissociated starch chains interacted with glycerol to form a V_h crystal structure.[39] The recrystallization of amylose and amylopectin during the drying of the FFS resulted in the semi-crystalline structure of the starch films.[23]

Rice starch (RS)/iota-carrageenan (ι-car) edible films exhibited a semi-crystalline structure.[57] The intensity of crystallite peaks decreased with the increase in the concentration of ι-car (0.50 to 2%), indicating that the addition of carrageenan significantly influenced the crystallinity of rice starch/iota-carrageenan/stearic acid films. According to the XRD results, the molecular interactions between RS and ι-car had a major impact on the properties of the film, limiting the miscibility and compatibility of mixed polysaccharides. Conversely, blending ι-car increased the crystallinity of AS films from 6.3 to 12.4%.[46] The observed increase is attributable to the blending of poorly crystalline nature AS (23.9%) and high crystalline ι-car (66.5%). The characteristic starch peak at 19.5° gradually flattened, and the peak at 28.35° increased with reducing starch and increasing carrageenan concentrations in the blend films.

XRD peaks of plasticized corn starch films prepared by two techniques, namely casting and twin-screw extrusion, were compared.[42] It has been observed that the formulation without extrusion showed a type A diffraction pattern of, with two major peaks at 2θ values of 18.5° and 23.2°, which are attributed to corn starch. Dual treatments did not influence the position of the peaks in the film; the peaks' intensity, however, decreased, which shows that the extrusion process might have caused partial gelatinization and fragmentation of the starch granules and transformed them into amorphous regions. The obtained results could lead one to conclude that the gelatinization of starch during the extrusion process and the addition of plasticizers could hinder the crystallinity. For banana peel starch-based thermoplastic films, diffraction peaks were detected at 2θ values of 17.2°, 20°, and 22.3°, suggesting the B-type starch polymorph.[49] The impregnation of banana peel nanocellulose fibers (BPNCFs) increased the overall crystallinity of the film from 20% to 48% due to the crystalline nature of BPNCFs.

The impact of the addition of a cross-linking agent on the crystallinity of the PS/CS blend films was reported in the literature.[48] The control film without a cross-linker showed three major diffraction peaks at 17.14°, 19.76°, and 22.14°, corresponding to the crystal lattice of chitosan and the type-B crystal structure of potato starch. The cross-linking reduced the diffraction peaks of the composite films, indicating restricted molecular chain movements and reduced crystallinity. A similar reduction in crystallinity has been reported for sweet potato starch-based films upon incorporation of sorbitol and mannitol as crosslinkers.[62] The addition of phenolic compounds, including protocatechuic acid, naringin acid, and tannic acid, did not influence the diffraction peak position, suggesting that homogeneous dispersion of phenolic compounds occurred in the film.[61]

The guar gum/nanochitosan/potato starch films showed changes in the X-ray diffraction patterns.[62] The starch films exhibited three sharp crystalline peaks at 16.8°, 19.3°, and 22.7°, whereas the blending of guar gum enhanced the intensity of the 16.8° and 22.7° peaks. The nanochitosan inclusion increased the crystallinity of the composite materials, which was attributed to the improved interfacial interactions between polymers and nanofillers. The incorporation of gelatin in the sweet potato starch-based edible film led to an increase in the crystallinity of the blend film.[63] The addition of CNCs and CNFs into the pumpkin starch film matrix slightly shifted the major diffraction peak from 19.6° to 18°, indicating the crystal structure transition from the V_h to the E_h form.[39] The absence of new

diffraction peaks in the nanocomposites indicates the miscibility of nanocellulose with starch chains.

XRD patterns of oxidized hydroxypropyl cassava starch showed two broad peaks at 7.6° and 20.6°, and a marginal peak at 13.8°, confirming the semi-crystalline structure of the starch-based films.[20] Upon the addition of CEO, the composite film displayed two new peaks at 24.5° and 30.1°, indicating the lipid cross-linking with starch in the film matrix. Moreover, the intensity of the characteristic peaks of starch increased and sharpened slightly, indicating an increase in the regular domains and crystallinity of the films. Therefore, the incorporation of CEO improved the structural stability and compatibility of the crystal structure of the films.

An active edible film prepared from sugar palm starch (SPS) and chitosan (CH) with extra virgin olive oil (EVOO) added displayed both broad and sharp peaks attributed to an amorphous and crystalline region, respectively, suggesting that the film is semi-crystalline in nature.[56] The crystalline peaks at 18° and 20° (2θ) correspond to A-type crystals, and the peak at 19° (2θ) was characterized by V-type crystals with an interaction of glycerol with the helices of a single amylose. No additional peak appeared with the addition of EVOO to the film, suggesting that the incorporation of EVOO in the CH/SPS-based blend film did not affect the structure of the CH/SPS film. In another study, the carvacrol and citral incorporated sago starch and guar gum blend films displayed two strong peaks at 9.6° and 28.75°. However, the addition of EOs had no impact on starch crystallinity.

The effect of fireweed extract on the crystallinity of corn starch (CS) films was studied.[23] The CS films showed diffraction peaks at 5.7°, 17.1°, 19.4°, and 21.7°, with peaks located at 17° and 19° attributed to the high-intensity amylose and amylopectin recrystallization during the storage of the film. The addition of an extract reduced the peak intensities due to the reduced retrogradation of starch. It has been reported that the intermolecular interactions between amylose/amylopectin chains and polyphenols prevent the reassociation of starch molecules into more ordered structures. The incorporation of NFC and NFCL in corn starch-based films led to a significant increase in the crystallinity of the film. The neat corn starch film showed a diffraction peak at 16.90°, which corresponds to B-type starch molecules. The conversion of corn starch from A-type to B-type occurred due to the plasticization and gelatinization of starch.[61]

8. Thermal properties

8.1 Differential scanning calorimetry (DSC)

Thermal analysis by DSC provides information on the melting temperature, glass transition temperature, and crystallization temperature of starch-based edible films. The concentration and type of plasticizers used in starch-based edible films have a significant impact on the thermal behavior, in particular lowering the glass transition temperature (T_g) by allowing chain mobility. A range of plasticizers has been used for making edible starch-based films. The impact of sorbitol and glycerol on the retrogradation of mung bean starch in the film matrix was studied.[11] The neat-starch films demonstrated two endothermic peaks at around 65 °C and 114 °C. Upon incorporation of plasticizers, only one endothermic peak appeared, while the second one disappeared. Furthermore, an increasing plasticizer concentration decreases the endothermic peak temperature and increases the range transition temperature (ΔT). The sorbitol-plasticized films showed higher peak temperatures than the glycerol-incorporated ones. These results indicate that the type of plasticizers and their concentration result in different interactions with the starch molecules.

An arrowroot starch (AS)/iota-carrageenan (IC)-based edible film showed glass transition (T_g) in the temperature range of 153 to 176 °C; however, the control film did not show any glass transition.[46] The control AS films exhibited two melting temperatures (T_m) at 167 °C and 190 °C. However, blending the AS with IC lowered the T_m to 153 and 176 °C with sharp peaks compared to the neat-starch films. In another study, DSC thermograms of PMS and PMS/CG films demonstrated the presence of a single endothermic peak, which indicates the miscibility of components in the melt.[33] The single endothermic peak has been attributed to the melting of crystalline amylopectin, which is further reorganized during retrogradation. The T_m of the neat PMS film was recorded to be 98 °C, which increased significantly to 118 °C for PMS/CG composite films. This might be attributed to the formation of a compact network in the polymer due to strong intermolecular interactions between PMS and CG. A similar increase in the endothermic peak from 82.3 to 122.2 °C was observed for the potato starch/chitosan composite films cross-linked with citric acid.[48] These results suggest that the cross-linking interactions hinder water evaporation from the film matrix.

The synergistic effects of the incorporation of oil and cross-linking on the thermal properties of pearl millet starch were studied.[64] The native starch films exhibited an endothermic peak of T_m at 168.39 °C with a melting enthalpy of 328.34 J g^{-1}, and the corresponding values for STMP cross-linking films were 172.63 °C and 358.20 J g^{-1}, respectively ($P < 0.05$). The improved thermal properties were attributed to strong intra- and intermolecular bond formation. The addition of EO to the cross-linked starch films facilitates chain mobility and further enhances the T_m and melting enthalpy to 185.68 °C and 498.38 J g^{-1}, respectively.

8.2 Thermogravimetric analysis (TGA)

The mass loss during heating in a higher range of temperatures provides information on the thermal stability of the film, as measured on a TGA. The addition of iota-carrageenan (IC) to arrowroot starch (AS) led to a reduction in the thermal stability of the films.[46] For the neat AS film, weight loss occurred in three stages during thermal scanning. The first stage occurred at temperatures ranging from 20 to 150 °C, which showed the evaporation of moisture, whereas degradation at 150 and 400 °C corresponded to starch degradation. The derivative TGA curves indicated that the IC and AS peak temperatures were 240 and 327 °C, respectively. However, the composite AS/IC films exhibited a lowering of thermal degradation temperature (297

to 281 °C). Furthermore, at the melting temperature, the weight loss of the composite films varied significantly from 50.51 to 62.90%. For banana peel thermoplastic (BPT) films, the first weight loss occurred at 150 °C attributable to the evaporation of free water, whereas the major mass loss happened at 290 °C, corresponding to starch degradation.[49] The addition of banana peel nanocellulose fibers (BPNCFs) in the BPT film improved the thermal stability of the film with an increase in degradation temperature of 15 °C.

The potato starch/chitosan blend films cross-linked with citric acid showed improved thermal stability.[48] The composite films had two stages of weight loss, at around 40 to 150 °C and 200 to 400 °C. Notably, the cross-linked films showed that the maximum degradation temperatures of both weight-loss stages increased gradually from 66.4 to 76.2 °C and 279.2 to 284.1 °C, respectively. The increase in the onset temperature was pronounced in cassava starch-based films cross-linked with ferulic acid due to structural changes in the polymer matrix.[66] A similarly enhanced thermal stability of CNC and CNF-incorporated pumpkin starch films has been reported.[39] The starch-based films showed three major steps of thermal decomposition. Compared to neat-starch films, the CNC and CNF additions reduced the mass loss in the second and third stages, which was attributed to the hydrogen bond interactions in the polymer matrix. Interestingly, the CNF-loaded films showed better thermal stability than CNC-based films, which might be associated with their larger particle size.

The effectiveness of nanofillers (nanochitosan) for the thermal stability of potato starch/guar gum composite films was studied.[62] The authors used T_{10} and T_{50} to represent mass losses of 10 and 50% during thermal scanning, respectively. Incorporating 2% nanochitosan into starch increased the T_{10} from 79.36 to 214.82 °C and significantly improved thermal stability. Similarly, other parameters were also improved by adding nanochitosan to the starch/gum composite matrix. These results could be useful for food packaging where thermal treatment or storage at elevated temperatures is desired.

The oxidized hydroxypropyl cassava starch (OHCS)/CEO films displayed weight loss in multiple steps in the TG and DTG curves.[20] The first weight loss (30 to 136 °C) was related to water evaporation, and the second mass loss (136 to 369 °C) was due to the degradation of starch, the decomposition of low molecular weight polymers, and the volatilization of Tween 80 and glycerol. The final degradation (369 to 600 °C) was attributed to the decomposition of stable components (volatile and non-volatile) in CEO. The incorporation of CEO reduced the major mass loss during heating, which indicates an enhancement in the thermal stability of the OHCS/CEO films. Similarly, the incorporation of *Mentha spicata* and *Cymbopogon martini* EOs increased the maximum degradation temperatures of arrowroot starch/carnauba wax nanoemulsion/cellulose nanocrystal films from 313.4 °C to 317.8 °C and 317.3 °C, respectively.[52] A change in the thermal degradation rate was observed for basil essential oil (BEO)/corn starch/CNF-based films with a change in the formulation. A lower concentration of corn starch (4% w/w) and BEO (2% w/w) resulted in a slower thermal decomposition rate when compared to the formulation containing higher corn starch (5% w/w) and BEO (3% w/w), respectively. This could happen because of the formation of cross-linking among corn starch, CNFs, and BEO in selected combinations, which affects the compactness of the film matrix, the mobility of the molecules, and finally, the thermal stability.[43] Three-stage weight losses were recorded for the starch and gelatin blend film. The first stage attributed to moisture loss occurred at 50 to 150 °C followed by the second stage, which ranged between 170 and 290 °C because of the loss of bound water and degradation of glycerol and volatile substances, whereas the final stage that occurred above 300 °C was due to the thermal decomposition of gelatin and starch. The incorporation of 10% resveratrol in the potato starch/gelatin film increased the peak temperature associated with the evaporation of water molecules from 98.86 to 115.24 °C, suggesting an interaction of resveratrol with starch and gelatin that restricted the evaporation of water molecules. However, the incorporation of resveratrol at 20% concentration increased the thermal degradation temperature of the starch/gelatin/resveratrol film by 6 °C compared to that of the neat potato starch/gelatin films, confirming an increase in the thermal stability.[45]

8.3 DMA

In addition to DSC, dynamic thermal mechanical analysis (DMA) is another technique that can be employed to identify relaxation temperatures associated with glass transitions and the macro-behavior of film materials resulting from changes in the microstructure of the film.[65] Many reports confirmed the great functionality of DMA in measuring the viscoelastic properties of starch-based films.

DMA of the starch/agar/maltodextrin films displayed a peak of $\tan\delta$, suggesting relaxation temperatures.[15] At sub-zero temperatures, two frequency-dependent relaxations, followed by relaxations at higher temperatures, were observed. These are common for plasticized polymers (Fig. 6). High-temperature relaxation contributes to increasing the mobility of molecules corresponding to the glass transition as α-relaxation. On the other hand, a lower temperature relaxation suggested vibration and rotation of side groups of polymer chains, indicating the local mobility of polymers. The inclusion of 10% agar improved the α-relaxation temperatures (T_α) and β-relaxation temperatures (T_β) of starch-based films. Due to the interaction between glycerol and agar, the plasticization effects within starch matrices were minimized, resulting in a higher T_β. A further increment in the concentration of agar slightly improved T_β. Furthermore, the mobility of local polymeric domains was restricted due to the interaction between starch and agar. T_α showed a less significant modification with an increased concentration of agar. Plasticized agar entangled the starch matrices at concentrations of 10% and above to form continuous networks, which dominated the phase transition behaviors in the blend of filmogenic materials. The thermal stability of the films is the key to selecting a packaging material based on the suitability of the developed edible films.[32] The resistance to temperature varies among food packaging materials, and mostly the starch-based edible films degrade at a temperature above 50 °C.[45,48,49]

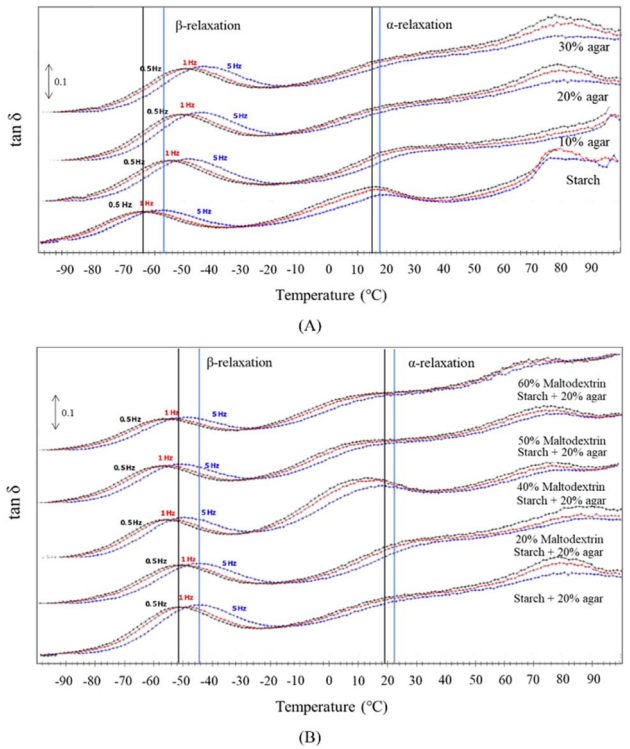

Fig. 6 DMTA analysis for temperature sweep at selected frequencies of 0.5, 1.0 and 5.0 Hz of starch films containing agar and maltodextrin at different concentrations; (A) agar concentrations of 0 (starch), 10%, 20% and 30% without maltodextrin and (B) maltodextrin concentrations of 20%, 40%, 50% and 60% at an agar concentration of 20%.[15]

9. Mechanical properties

Measuring the mechanical properties of biopolymeric edible films is very important as they provide an indication of their strength and structure. The mechanical properties of the films are commonly measured and represented in terms such as tensile strength (TS), elongation at break (EAB), and Young's modulus (YM). An increased crystallinity in starch can lead to a more rigid and less flexible film with poor barrier properties. It is furthermore noticed that water activity and relative humidity affect the mechanical properties of the films derived from starch due to the strong intrinsic affinity of starch molecules towards water, which absorb water at higher humidity, and the absorbed water induces a plasticization effect, reducing the mechanical properties of the film. The mechanical properties of starch-based edible films can be modified or controlled by blending the starch-based films or coatings with different biopolymers such as gums, cellulose derivatives, or chitosan to overcome the limitations.[17,66] The mechanical properties of several starch-based edible films are presented in Table 1.

A comparative study of the mechanical properties among five selected starch-based edible films (*e.g.*, tapioca, potato, corn, wheat, and rice) with glycerol as the plasticizer was reported.[67] Tapioca films exhibited the maximum TS compared to other films, followed by potato starch films. Both of these films also exhibited superior EAB. Films produced from rice starch had a moderate TS and a higher EAB. Corn starch films and wheat starch films had the least mechanical properties.

The concentration and type of plasticizers largely affect the mechanical properties of starch-based edible films. The effect of mung bean starch concentration (3.5–5%), and two selected plasticizers and their concentrations [sorbitol (0–60% w/w) and glycerol (0–30% w/w)] on the mechanical properties of mung bean starch-based films was investigated.[11] The results showed that the starch concentration did not cause any remarkable differences in the properties of the film. Starch films without plasticizers showed the highest TS and elastic modulus (EM) but low flexibility due to the cohesive forces of amylose chains within the film matrix. The addition of a plasticizer increased the polymer chain's mobility and free volume by establishing intermolecular interactions with starch molecules, enhancing flexibility and lowering film brittleness. On increasing plasticizer concentration, the TS and EM were reduced; however, the EAB increased. Glycerol demonstrated a better plasticization effect than sorbitol in the mung bean starch-based films due to their low molecular weight and smaller size. Increasing plasticizer (*e.g.*, glycerol or sorbitol) concentration decreased TS and EM but increased EAB because of the increased chain mobility.

A high concentration of easily deformed amorphous starch in the matrix is a plausible reason for the poor mechanical properties of starch-based films. To overcome such limitations, several researchers have proposed the blending of two or more biopolymers so that the resultant starch-based blend film can possess improved mechanical properties. A blend of 4% AS and iota carrageenan (0.2–2%) produced a blend film that showed an increase in TS up to 92% and a drop in EAB by half when compared to the neat starch film.[46] Similarly, blending iota-carrageenan with rice starch increased the TS dramatically from 31.6 to 116.5 N m^{-2}, and the corresponding EAB also increased from 15.7 to 45.6%.[57] The enhanced mechanical properties of carrageenan-blended starch films are attributed to the compact matrices obtained during the gelation of carrageenan helices, which form a 3D structure associated with paired chains of starch and carrageenan.

Adding agar to starch can enhance the mechanical properties of the blended films.[15] A 30% agar addition increased the TS and YM by 2.5 and 5 times, respectively; however, it reduced the EAB. The rigid agar polymer created cage-like networks *via* intermolecular hydrogen bonding interactions stabilized by anhydro-L-galactopyranosyl residues, reducing flexibility and increasing stiffness. Furthermore, adding low molecular weight maltodextrin to starch plasticizes the blend network, reducing the TS, EAB, and YM of the starch/agar/maltodextrin films. Similarly, increasing the concentration of pearl millet starch and carrageenan gum enhanced the TS; however, increasing glycerol concentration reduced the TS of composite films.[33] Conversely, the bilayer films made using corn–wheat starch and zein showed an increment in EAB and a reduction in TS.[44] Moreover, by varying the starch concentration, there were no significant differences in the EAB and TS of bilayer-films.

The cross-linking of starch has been proven to improve the mechanical properties of starch-based edible films. It has been reported that both TS and YM of the mung bean starch (MBS)

Table 1 Mechanical properties of starch-based edible films

Biopolymer	Additives	Processing conditions	Tensile strength (MPa)		Elongation at break (%)		Young's modulus (MPa)		Reference
			Control	Modified	Control	Modified	Control	Modified	
Mung bean starch	Sorbitol and glycerol	Starch: 5% Heating: 85 °C for 30 min Additives: 0 to 60% Drying: 35 °C for 20 h	46.30	7.14	2.46	56.95	1428.45	16.29	11
Mung bean starch	Citric acid	Starch: 3.5 to 5% Heating: 85 °C for 1 h Additives: 0 to 15% Drying: 30 °C for 16 h	7.34	13.98	36.00	16.94	346.18	687.71	58
Arrowroot starch	Iota-carrageenan	Starch: 4% Heating: 70 °C for 5 min Additives: 0 to 50% Drying: 50 °C for 6 h	0.17	2.20	72.62	32.65	—	—	46
Corn starch	Fireweed extract	Starch: 4% Heating: 80 °C for 30 min Additives: 0 to 0.05% Drying: 25 °C for 24 h	3.78	4.50	60.09	63.64	95.25	114.73	23
Faba bean starch	Sodium trimetaphosphate	Starch: 4% Heating: 80 °C for 1 min Additives: 1 to 5% Drying: 50 °C for 16 h	8.25	14.28	39.27	25.62	—	—	73
Pumpkin starch	Cellulose nanocrystals	Starch: 3% Heating: 100 °C for 30 min Additives: 0 to 2% Drying: 35 °C for 10 h	3.95	6.23	58.83	61.75	—	—	74
Banana starch	Curcumin loaded orange oil nanoemulsion	Starch: 3% Heating: 80 °C for 1 h Additives: 0 to 0.2% Drying: 35 °C	23.01	2.18	2.03	6.09	—		71
Pearl millet starch	Sodium trimetaphosphate and fenugreek oil	Starch: 4% Heating: 80 °C for 20 min Additives: 0.80 g Drying: 45 °C for 24 h	3.44	4.59	56.5	61.5	—	—	64
Cassava starch	Cinnamon essential oil	Starch: 5% Heating: 70 to 80 °C Additives: 0 to 2.5% Drying: 40 °C for 12 h	2.08	0.80	3.52	42.17	—	—	20

Table 1 (*Contd.*)

Biopolymer	Additives	Processing conditions	Tensile strength (MPa)		Elongation at break (%)		Young's modulus (MPa)		Reference
			Control	Modified	Control	Modified	Control	Modified	
Potato starch	Zedo gum and *Salvia officinalis* essential oil	Starch: 5% Heating: 90 °C for 30 min Additives: 0 to 1.5%; 0 to 500 μL Drying: 60 °C for 18 h	4.72	1.62	98.97	34.22	—		51
Banana peel starch	Banana peel nanocellulose	Starch: 7.5% Additives: 0 to 5% Drying: 40 °C for 24 h	5.10	30.89	101.51	90.29	5.02	34.21	49
Chayote tuber starch	Zein–pectin nanoparticle-stabilized cinnamon essential oil Pickering emulsion	Starch: 4% Heating: 90 °C for 25 min Additives: 0 to 4% Drying: 45 °C for 15 h	5.44	2.59	45	70.8	—	—	50
Sweet potato starch	Mannitol and sorbitol	Starch: 15% Heating: 90 °C for 30 min Additives: 30% Drying: 40 °C for 15 min	11.40	19.73	0.96	2.80	—	—	75
Corn starch	Ethanolic extract of propolis and *Thymus vulgaris* essential oil	Starch: 3% Heating: 60 °C for 50 min Additives: 10%; 2% Drying: 20 °C for 48 h	16.1	7.8	5.8	13.5	452	317	76
Dioscorea zingiberensis C. H. Wright starch	Oregano essential oil	Starch: 6% Heating: 90 °C for 30 min Additives: 0 to 3% Drying: 35 °C for 24 h	10.96	3.15	109.40	100.11	—	—	55
Potato starch	*Viola odorata* extract	Starch: 4% Heating: 85 °C for 30 min Additives: 0 to 3% Drying: room temperature	39.84	36.67	11.09	12.39	296.72	286.44	72
Potato starch	Gelatin and anthocyanins from purple sweet potato	Starch: 4.5% Heating: 85 °C for 30 min Additives: 0 to 2% Drying: 35 °C to 36 h	8.86	13.99	72.22	48.89	—	—	77

edible films cross-linked with citric acid (CA) improved, and the corresponding EAB decreased.[58] On addition of 3% CA to starch achieved the optimum mechanical properties of the films with TS, YM, and EAB values of 13.98 MPa, 687.79 MPa, and 16.94 ± 0.35%, respectively, suggesting that an efficient cross-linking occurred between MBS and CA. However, increasing the CA concentration to 15% did not improve the TS or YM. At higher concentrations of CA (10 and 15%), the films showed higher EAB and lower YM than control MBS films, attributed to the plasticizer effect of CA. Similarly, a 29% increase in TS and a 57% increase in EAB were reported for potato starch/chitosan films cross-linked with CA.[48] The incorporation of ferulic acid significantly increased the TS and reduced the EAB of the cassava starch-based film compared to the native starch-based film due to a modification in the crosslinking interaction between polymeric chains.[68] Sodium trimetaphosphate (STMP) cross-linked faba bean starch films demonstrated enhanced TS compared to the native starch films.[38] The TS of the native starch film was 8.25 MPa, which increased to 10.96, 12.77, and 14.28 MPa upon the addition of 1, 3, and 5% STMP, respectively. Furthermore, by increasing the concentration of the cross-linking agent from 1 to 5%, it was found that the EAB decreased significantly from 35.11 to 25.62%.

Incorporating CNCs and CNFs increased the TS and EAB of the pumpkin starch-based films.[39] It has been observed that CNCs act as a better reinforcement agent than CNFs, which is attributed to the high elastic modulus and large surface area of the CNCs, which enhanced the interfacial interactions within the starch matrix. The incorporation of CNFs from banana peel significantly improved the TS of BPT films from 5.10 MPa to 30.89 MPa.[49] The addition of nanofibrillated cellulose (NFC) and nanofibrillated lignocellulose (NFLC) to corn starch significantly increased the tensile index of blend films from 8.66 N m g^{-1} to 12.32 N m g^{-1} and 10.55 N m g^{-1} respectively. On the other hand, the addition of NFC and NFLC remarkably reduced the burst index compared to that of the neat corn starch film.[61] The incorporation of nanochitosan into potato starch/guar gum composite films increased both the TS and EAB.[62] In a separate study, the CNC incorporation increased the TS to 76% and reduced the EAB by 96% compared to those of the control arrowroot starch/carnauba wax nanoemulsion films.[52] However, the high-amylose corn starch (HACS)-based composite film with the added quinoa cellulose nanocrystal (QCNC) showed lower TS than the neat HACS film. This was due to the poor compatibility of the QCNC with HACS and higher intramolecular bonding than intermolecular bonding, leading to phase separation, which subsequently reduced the TS. The EAB of the HACS/QCNC films significantly increased with the addition of the QCNC.[69]

Adding cinnamon essential oil (CEO) to cassava starch significantly increased EAB and reduced the TS of the blended films.[20] The TS of the CEO-loaded films was influenced by the substitution of strong polymer–polymer intermolecular interaction by the weaker polymer–oil interaction. Moreover, CEO imparted a plasticization effect by increasing the polymer chain mobility, thereby enhancing the flexibility of the films. Similarly, loading *Salvia officinalis* essential oil in potato starch/Zedo gum blended films reduced TS and EAB.[51] Incorporation of zein–pectin nanoparticle-stabilized cinnamon essential oil Pickering emulsion (ZPCO) in the chayote tuber starch (CTS)-based film significantly reduced the TS and increased the EAB as compared to those of the neat CTS film.[50] The neat-starch film exhibited the highest TS of 4.72 MPa and EAB of 98.97%, whereas the addition of gum and EO linearly reduced the mechanical properties. The high water-absorbing properties of Zedo gum increased the moisture content; this moisture acts like a plasticizer and weakens the strong interactions between polymer chains.

Edible films prepared with carvacrol and citral loaded sago starch/guar gum demonstrated increased flexibility with reduced TS and Young's modulus (YM).[19] The addition of carvacrol and citral EOs reduced YM because oil reinforcement created chemical interactions with the starch chains within the biopolymeric architecture, forming a heterogeneous structure that promotes discontinuities and reduces stiffness. The incorporation of EO affects the interaction between the polymer–polymer chains, provides a bendable/flexible zone in the film matrix, and enhances the EAB value.[70] A similar observation was reported with the addition of OEO to the DZW starch-based film: the TS of the films decreased, and the corresponding EAB of the films increased when compared to that of the neat DZW starch-based film.[56] The banana starch and curcumin-loaded orange oil nanoemulsion edible films demonstrated a lowering of the TS (2.18 MPa) and an increment in the EAB (6.09%) when compared to the neat starch films (TS: 23.01 MPa and EAB: 2.03%).[71] The presence of oil and surfactants in the nanoemulsions disrupted the existing intermolecular interactions, thereby increasing the flexibility of the films with a reduction in their resistance.

Adding fireweed extract (0.05%) to corn starch increased the TS, EAB, and YM to 19, 6, and 20%, respectively, compared to the neat-starch films.[23] The addition of epigallocatechin gallate (EGCG), blueberry ash fruit extract (BBA), and macadamia peel extract (MAC) at lower concentrations in the pea starch/guar gum blended film significantly reduced TS and YM, and increased EAB.[16] However, further increases in EGCG, BBA, and MAC extract concentrations improved the TS of the film from 27.8 to 38.8, 40.7, and 43.1 MPa, respectively. A similar trend was observed for the EAB and YM of the blend films. The hydroxyl groups of phenolic compounds interacted with the polymers *via* hydrogen bonding. The differences in the mechanical properties between lower and higher concentrations are attributable to the plasticizing and anti-plasticizing effects of the phenolic compounds in the polymer matrix. The addition of phenolic compounds (*e.g.*, resveratrol) has the potential to improve the mechanical properties of starch/gelatin-based edible films.[45] A potato starch/gelatin film enriched with resveratrol has significantly improved mechanical properties compared to the neat potato starch/gelatin film by increasing the TS from 3.99 ± 0.46 MPa to 5.45 ± 0.48 MPa. The corresponding EAB increased from 19.49 ± 0.98% (control) to 55.86 ± 1.50% (with 10% resveratrol). A similar increase in TS was observed after the incorporation of broccoli leaf polyphenols (BLPs) in the tapioca starch/pectin (TSP)-based film as

Table 2 Water vapor barrier properties of starch-based edible films

Biopolymer	Additives	Working conditions	Water vapor permeability ($g\ m^{-1}\ s^{-1}\ Pa^{-1}$)		Reference
			Control	Modified	
Cassava starch	Citric acid	RH: 70% Interval: 24 h Total duration: 10 days	2.8×10^{-10}	1.8×10^{-10}	59
Wheat and corn starch (3 : 2)	Zein	RH: 75%	8.89×10^{-11}	5.96×10^{-11}	44
Arrowroot starch	Iota-carrageenan	RH: 75% Temp: 25 °C Interval: 24 h Total duration: 7 days	3.06×10^{-11}	2.50×10^{-11}	46
Proso millet starch	*k*-Carrageenan	RH: 75% Temp: 30 °C	3.19	2.38	47
Faba bean starch	Sodium trimetaphosphate	—	1.34	1.10	73
Pearl millet starch	Sodium trimetaphosphate and fenugreek oil	RH: 75% Temp: 30 °C Interval: 3 h Total duration: 48 h	6.98	8.76	64
Banana starch	Curcumin loaded orange oil nanoemulsion	RH: 65% Temp: 25 °C Interval: 1 h Total duration: 8 h	2.12×10^{9}	0.78×10^{9}	71
Corn starch	Fireweed extract	Area: 0.0050 m^2 RH: 50% Temp: 25 °C Interval: 2 h Total duration: 10 h	5.81×10^{-10}	6.00×10^{-10}	23
Mung bean starch	Glycerol and sorbitol	Area: 0.000777 m^2 RH: 100% Interval: 12 h Total duration: 7 days	0.56×10^{-10}	1.31×10^{-10}	11
Mung bean starch	Citric acid	RH: 50% Temp: 25 °C Interval: 2 h Total duration: 2 days	2.86×10^{-12}	2.65×10^{-12}	58
Cassava starch	Cinnamon essential oil	RH: 100% Temp: 25 °C Interval: 2 h Total duration: 12 h	1.04×10^{-14}	1.90×10^{-14}	20
Potato starch	Zedo gum and *Salvia officinalis* essential oil	Area: 0.0019625 m^2 RH: 75% Temp: 25 °C	9.53×10^{-11}	5.58×10^{-11}	51
Cassava starch	Sodium tripolyphosphate, sodium phosphate, and ferulic acid	RH: 75% Temp: 20 °C Total duration: 12 h	2.47×10^{-10}	1.74×10^{-10}	68
Chayote tuber starch	Zein–pectin nanoparticle-stabilized cinnamon essential oil Pickering emulsion	RH: 90% Temp: 25 °C Interval: 24 h Total duration: 7 days	1.77×10^{-10}	1.24×10^{-10}	50
Sweet potato starch	Mannitol and sorbitol	Area: 0.0033 m^2 RH: 90% Temp: 38 °C	9.84×10^{-11}	4.31×10^{-11}	75
Corn starch	Ethanolic extract of propolis and *Thymus vulgaris* essential oil	Area: 0.0031 m^2 RH: 60% Temp: 25 °C	9.17×10^{-11}	10.07×10^{-11}	76
Dioscorea zingiberensis C. H. Wright starch	Oregano essential oil	Area: 0.0028 m^2 RH: 50% Temp: 25 °C Interval: 1 h Total duration: 12 h	0.86×10^{-9}	1.11×10^{-9}	55
Potato starch	*Viola odorata* extract	RH: 55% Temp: 25 °C	6.6×10^{-4}	5.7×10^{-4}	72

Table 2 (*Contd.*)

Biopolymer	Additives	Working conditions	Water vapor permeability ($g\ m^{-1}\ s^{-1}\ Pa^{-1}$) Control	Modified	Reference
Potato starch	Gelatin and anthocyanins from purple sweet potato	RH: 100% Temp: 25 °C Interval: 24 h Total duration: 7 days	6.92×10^{-11}	6.27×10^{-11}	77

compared to the control film, whereas the EAB of the TSP/BLP-based composite film was reduced as compared to that of the control TSP film.[54] On incorporation of 3% *Viola odorata* extract (VOE) in the potato starch-based film, the TS of the film was significantly reduced from 39.84 to 36.67 MPa. Moreover, the EAB of the film was found to have increased from 11.09 to 12.39% due to the weakening of intermolecular forces caused by the phenolic compounds of VOE.[72] Generally, for the protection of packaged food from external forces, the packaging material must exhibit a good TS, EAB, and resistance to puncture. This enables the loss-free distribution of packaged food products during storage and transportation by providing a significant level of protection.

10. Barrier properties

Barrier properties are the central core of packaging materials, whether edible or non-edible. Mostly, barrier properties are used to measure the resistance of the films towards light, water, and oxygen. The water vapor transmission rate (WVTR) and the oxygen transmission rate (OTR) are the widely measured barrier parameters of films; furthermore, these results are processed and represented as water vapor and oxygen permeability data.

While comparing the water vapor permeability (WVP) of five selected starches (*e.g.*, wheat, corn, rice, tapioca, and potato), it was observed that the corn starch-based film and tapioca starch-based film had the lowest and highest WVP values, respectively.[67] Subsequently, rice and wheat starch films showed comparable values of WVP to the corn starch film. The observed difference could be related to a large difference in their amylose contents. The corn, wheat, and rice starches contain significant amounts of amylose (25–30%), whereas potatoes and tapioca have moderate amounts of amylose (16–21%). Furthermore, the enhanced WVP might also be attributed to the high lipid contents of wheat, corn, and rice starches. The WVP values of various starch-based edible films are tabulated in Table 2.

The type of plasticizer and concentration of starch significantly varied the oxygen and water vapor barrier properties of the mung bean starch-based films.[11] The increase in starch concentration from 3.5 to 5% decreases the WVP, which is attributed to the increased dissolved solids in the film-forming solution. Conversely, the WVP increases with an increase in plasticizer concentration due to the restricted intermolecular interactions among polymer chains and enhanced free volume in the plasticized film matrix. Nevertheless, the addition of plasticizers in the mung bean starch films reduced the oxygen permeability (OP). The sorbitol-plasticized films showed lower OP than the glycerol-plasticized starch films.

Blending starch with hydrophobic agar improved the water vapor and oxygen barriers significantly.[15] The addition of agar by up to 20% reduces the free volume and adjacent space for molecular diffusion. An increasing agar concentration improved both WVP and OP, indicating aggregation and non-homogeneity of the agar that caused phase separation and enhanced vapor diffusion. On the other hand, maltodextrin addition plasticized and decreased the relaxation temperatures of blend films, which enhanced the molecular mobility and increased the diffusion of oxygen molecules. Nanocellulose fiber addition to BPT films significantly improved the oxygen barrier properties with the reduction of the oxygen transfer rate from 12.70 to 9.43 $cm^3\ \mu mm^{-2}\ d^{-1}\ kPa^{-1}$.[49] Similarly, the incorporation of NFC and NFLC into the corn starch-based film reduced the water vapor transmission rate (WVTR) significantly by improving the barrier properties of the film against water vapor.[61] Furthermore, the addition of quinoa cellulose nanocrystals (QCNCs) to the high amylose corn starch (HACS)-based film demonstrated an improvement in water barrier properties by lowering WVP values as compared to that of the control HACS film.[70]

A blended film made with an optimized formulation of 2% rice starch, 2% iota-carrageenan, and 0.3% stearic acid had the minimum WVP ($3.55 \times 10^{-11}\ g\ m^{-1}\ s^{-1}\ Pa^{-1}$).[57] The molecules of starch are assumed to be protected by the double helical structure of carrageenan, which traps them in a coiled shape. A similarly enhanced WVP was reported for the arrowroot starch/iota carrageenan blend films compared to the neat-starch films.[46] Conversely, the addition of *k*-carrageenan to Proso millet starch increased the WVP from 2.38 to 3.19 $g\ m^{-1}\ s^{-1}\ Pa^{-1}$, attributed to the hydrophilic nature of these blends.[47] A similar increase in WVP was also reported for the guar gum-added potato starch films.[62]

The WVP of the neat PMS and PMS/CG blended films ranged from 0.65×10^{-10} to $3.31 \times 10^{-10}\ g\ m^{-1}\ s^{-1}\ Pa^{-1}$.[33] On increasing the concentration of PMS and CG, the WVP of PMS/CG-based composite films decreased, which might be associated with increased crosslinking. Furthermore, higher gum and starch concentrations improve the chain-to-chain interaction in polymers, resulting in stronger films with lower gas and water permeability. Similarly, the addition of a zein layer to the corn/wheat starch blend films reduced WVP from 8.89×10^{-11} to

5.96×10^{-11} g m^{-1} s^{-1} Pa^{-1}.[44] The hydrophobicity of the zein molecules led to a low affinity for water, attributed to the reduced WVP of bilayer films. In addition, the surface defects with holes in the starch films showed higher WVP, whereas the introduced zein occupied the gaps and led to a compact microstructure with an enhanced water vapor barrier.

Citric acid-assisted cross-linking has significantly reduced the WVP of starch-based films; however, the permeability showed a concentration dependency on CA.[78] For plasticized corn starch films, the addition of CA (0–20% w/w) caused a significant decrease in the WVP of the films. An addition of 10% CA to plasticized CS decreased the WVP from 1.28×10^{-10} to 0.73×10^{-10} g m^{-1} s^{-1} Pa^{-1}, which might be attributed to the substitution of hydrophilic OH groups with hydrophobic ester groups. However, increasing the CA content to 20% negatively affected the barrier properties of the cross-linked films by increasing the value from 7.28×10^{-11} to 8.56×10^{-11} g m^{-1} s^{-1} Pa^{-1}, which is attributed to the plasticization effect of excess CA by enhancing the interchain and space chain mobility that accelerates water vapor diffusivity through the film. This is in agreement with the films made by CA-assisted cross-linking of mung bean starch (MBS), where the CA concentration was, however, significantly lower (3%).[58] A similar effect was present for the CA cross-linked potato starch/chitosan films.[48] Ferulic acid, as a crosslinker, lowered the WVP of cassava starch-based films compared to native starch-based films.[68] The WVP was reduced up to 32% for the composite films with 15% CA due to the partial replacement of hydrophilic hydroxyl groups with hydrophobic ester groups. However, the WVP slightly increased for 20% CA-incorporated films, attributed to the plasticizing effect of CA that could have increased the mobility of interchain molecules. The incorporation of sodium trimetaphosphate (STMP) as a cross-linking agent has also improved the water vapor barrier of the faba bean starch films.[38]

The oxidized hydroxypropyl cassava starch-based edible films incorporated with cinnamon essential oil (CEO) demonstrated that the increasing concentration of CEO affected the WVP of the films.[20] The increase in concentration of CEO from 0 to 2.5% resulted in increased WVP values from 1.04×10^{-10} to 1.90×10^{-10} g m^{-1} s^{-1} Pa^{-1}, which could be related to CEO's detrimental effects on the film microstructure, the creation of holes and micropores in the film's structure, and the diffusion of water vapor molecules as a result. Conversely, the oxygen barrier properties increased marginally when the concentration of CEO increased from 0.5% to 1.5%. Such an increase might be due to the presence of Tween 80 and its emulsification effect, which made CEO better exist and stabilize in the film and prevented phase separation in the system. Furthermore, the compatibility between the film matrix and CEO results in a compact structure, which may prevent the transmission of non-polar oxygen molecules through the film matrix. The addition of OEO (1 to 3%, w/w) into the DZW starch-based film increased the WVP values from 0.86×10^{-9} g m^{-1} s^{-1} Pa^{-1} (without OEO) to 1.11×10^{-9} g m^{-1} s^{-1} Pa^{-1} (with 3% OEO). The reduction in WVP is related to the creation of micropores, as observed through the SEM microstructure of the films.[55] The decrease in WVP in ZPCO/CTS films occurred due to the creation of a tortuous inner pathway, making it difficult for water molecules to pass through the film matrix.[50] Similarly, the incorporation of both citral and carvacrol synergistically increased the water vapor barrier of the sago starch/guar gum films.[19]

The addition of plant extracts to starch-based edible films improved the water vapor barrier properties. The pea starch/guar gum composite films loaded with MAC and BAN significantly reduced the WVP from 13.87×10^{-10} to 7.05×10^{-10} and 7.39×10^{-10} g m^{-1} s^{-1} Pa^{-1}, respectively.[79] However, the incorporation of EGCG and BBA at 1.5 mg mL^{-1} concentration significantly increased the WVP to 16.49×10^{-10} and 14.99×10^{-10} g m^{-1} s^{-1} Pa^{-1}, respectively. The high-water absorption ability of phenolic compounds plasticizes the polymer chains, which increases the WVP of the active films. Similarly, the incorporation of fireweed extract (0.0125 to 0.05%) increased the WVP of corn starch (CS) films from 5.81 to 6.00×10^{-10} g m^{-1} s^{-1} Pa^{-1}.[23] Interestingly, the methylcellulose (MC) films with the same concentration of fireweed extract exhibited a comparatively higher WVP than corn starch films. A higher hygroscopicity and the repeating side chains containing –CH_3 groups in the cellulose chains of MC could be the reasons for the higher WVP. On the other hand, the CS films' superior water vapor barrier properties may be due to their more compressed structure created during the retrogradation process. The addition of resveratrol to the potato starch/gelatin film improved the water vapor barrier properties significantly by reducing the WVP values from 4.00×10^{-10} g m^{-1} s^{-1} Pa^{-1} (control potato starch/gelatin film) to 3.61×10^{-10} g m^{-1} s^{-1} Pa^{-1} (5% resveratrol added potato starch/gelatin film). This reduction in the WVP value was due to the lipophilic nature of resveratrol, which makes the film more hydrophobic, and the creation of a hindrance in the diffusion pathway of water vapor across the film.[45] A similar trend was observed while incorporating the VOE in the potato starch film at different concentrations.[72] The WVP value significantly decreased from 5.7 to 6.6×10^{-4} g m^{-1} s^{-1} Pa^{-1} on the incorporation of VOE at 3% concentration due to crosslink formation between the starch polymer, plasticizer, and phenolic groups of VOE. Furthermore, the TSP film with added BLPs showed a significantly lower WVP value as compared to the neat TSP film.[54] For the extension of the shelf-life of packaged food products, the WVP of edible films plays an important role in preventing moisture loss and gain in packaged food products.[26] The water vapor may transfer from the internal or external environment through the packaging film, which may result in a reduction in food shelf-life and its deterioration.[30,31] However, the required WVP value for the preservation of food products may vary depending on the type of packed food and its susceptibility to moisture.[80]

11. Patents on starch-based edible films and coatings

A patent is an exclusive right awarded to an inventor for an invention that could be a new product or a processing technology. Similar to other fields, several patents have been granted

Table 3 Patents on starch-based edible packaging materials

Title	Starch type	Other components	Application number	Reference
A kind of preparation method of a starch base edible film	Corn starch	Cellulose, glycerin, gellan gum, sodium alginate, sodium citrate, and organic acids	CN107011544A	81
A kind of starch-based edible inner packing film and the preparation method thereof	Amylose	Gluten, cellulose derivative, vegetable wax, emulsifier, and plasticizer	CN108250493A	82
High tensile strength composite polysaccharide edible film and the preparation method thereof	Potato starch	Sodium alginate, sodium carboxymethyl cellulose, and succinic anhydride	CN111808333A	83
A kind of edible packing membrane and the preparation method thereof with a high-barrier function	Wheat and corn	Chitin modified polypeptide hydrogel, nanocellulose, carrageenan, ethyl cellulose, maltitol, aluminium–magnesium silicate, and talcum powder	CN108752645A	84
Edible packaging film and the preparation method and applications thereof	Hydroxypropyl starch	Pullulan, ferulic acid, glycerol, and lemongrass oil	CN109438772B	85
A method of edible film preparation using oxidized starch	Corn starch	Sorbierite, citric acid, acetylation mono fatty-acid glyceride, and emulsifier	CN109294000A	86
Methods for preparing food packaging films with antibacterial activity, and applications thereof	High amylose corn starch	Konjac glucomannan, glycerin, perilla oil, and cyclodextrin	AU2019271993B2	87
Preparation method of antioxidant *Cyperus esculentus* starch composite edible films	*Cyperus esculentus* starch	Thymol and glycerol	CN114736436A	88
A kind of environment friendly degradable edibility edible film packaging material	Modified starch	Dandelion extract, konjaku rubber powder, gelatin, modified casein, carboxymethyl cellulose, chitosan, plasticizer, agar, citric acid, antimicrobial fluid, plant extract, carrot meal, cactus juice, and rice juice	CN109054105A	89
Biodegradable edible plastic container	Any combination of corn, potato, tapioca, wheat, rice, or equivalents	Acetic acid, citric acid, glycerin, agar, collagen, and thyme oil	WO2020018480A1	90
Edible beverage packaging bottle and the preparation method thereof	Potato starch	Edible oil, edible vinegar, edible wheat bran fiber, seaweed, and pineapple fiber	CN110817089A	91
New edible film using seaweed and the process of manufacturing thereof	Potato starch	Seaweed, agar, and soy lecithin	KR102261416B1	92

for innovations in starch-based packaging. Selected patents granted recently in the area of starch-based edible packaging materials intended for food packaging are listed in Table 3. A starch-based edible film preparation method with high transparency, good mechanical strength, and oxygen resistance was awarded a patent.[81] There are two steps in film preparation. In the first step, cornstarch, cellulose, and glycerine were blended together in aqueous solutions in the temperature range of 40 to 50 °C, resulting in liquid A. On the other hand, gellan gum, sodium alginate, and sodium citrate were blended in aqueous solutions at 40 to 50 °C to produce liquid B. Both liquids were mixed together at a pH of 6 to 7. Organic acids, lecithin, and lactose were added to the blend with continuous stirring and high-pressure homogenization. The mass was transferred into a film by casting, followed by drying.

In a separate patent, starch-based edible inner packing films were developed for packing instant noodles, coffee, bread, cake, and candy.[82] The film consists of gluten, a reinforcing agent (sodium carboxymethyl cellulose and microcrystalline cellulose), vegetable wax (from sugarcane and rice bran), an emulsifier (stearic acid), and a plasticizer (sorbitol and ethylene glycol). The prepared films exhibited a a tensile strength of 34–40 MPa, an elongation at break of 22–25%, light transmittance of 73–80%, and a vapor transmission coefficient of 0.09–0.11 g m^{-2} h^{-1} kPa^{-1}.

A high-tensile strength (>48 MPa) starch edible film was patented.[83] The porous starch sample was esterified by adding succinic anhydride, followed by compounding with sodium alginate and sodium carboxymethyl cellulose. In addition, the gelatinized starch paste was treated with ultrasound for 0.5–2 h.

This process greatly reduced the film-forming time, with an improved tensile strength of 48.8 to 54.5 MPa. One patent was registered on the preparation of starch-based edible films with improved barrier properties.[84] The cross-linked starch was compounded with nanocellulose, carrageenan, ethyl cellulose, maltitol, aluminum-magnesium silicate, and talcum powder. The mixture was shredded and then extruded at 145–165 °C using a twin-screw extruder. A chitin-modified polypeptide hydrogel was the reinforcing agent used to improve the barrier properties of starch films.

The hot pressing method was employed to prepare starch-based edible films with superior mechanical properties, flexibility, moisture, and oxygen barrier properties.[85] The prepared edible films were used as seasoning bags that can be cooked together with the packed products. The starch was mixed with pullulan, ferulic acid, glycerol, and lemongrass oil and heated at 70 °C for 1 h. The mixture was equilibrated overnight, followed by a two-step hot pressing process (130 °C, 2 MPa for 1 min, and 140 °C, 4 MPa for 5 min). In another invention, a unique drying process for starch films has been performed at 37–38 °C for 20–30 min.[86]

A low-calorie, edible packaging film with antibacterial activity was patented. The film was prepared by mixing corn starch, konjac glucomannan (a rich source of dietary fiber), and cyclodextrin-entrapped perilla oil.[87] The addition of konjac glucomannan to the starch chains hindered the brittleness and low ductility of the starch films. Encapsulation of oil using cyclodextrin regulates the release, improves solubility, and controls the volatilization of oil. The prepared composite film exhibited improved tensile strength and elongation at break, and reduced transparency and coefficient of moisture permeability compared to neat starch films. Furthermore, breads packed with the composite films showed a reduction in bacterial and mold growth. To impart antioxidant activities to the *Cyperus esculentus* starch edible films, a preparation method was invented.[88] Thymol was added to the gelatinized starch solution, which enhanced the DPPH radical scavenging activity (25–73%) of the films.

Hefei Technology[89] reported their innovation in the preparation of edible, non-toxic, oxygen-resistant, waterproof, high-temperature, and oil-resistant films. Starch was modified using a phosphate solution under heating and continuous stirring. It was further cross-linked with dandelion extract (natural rubber) and its hydrogen bonding was improved with carboxymethyl cellulose and agar incorporation. Modified casein was added to improve the oxygen barrier properties. The inclusion of plant extract and essential oil imparted antimicrobial activity to the prepared edible films.

Edible starch-based flexible films were made into a single-use container to pack nutritional supplements for sports activites.[90] The starch was compounded with acetic acid, citric acid, glycerin, agar, collagen, and thyme oil and heated at 160–195 °C to form a gel. The gel was further dried to obtain flexible films. The films were shaped into containers that can be torn off with teeth and are edible.

One patent was reported on an edible protection film made of potato starch that was attached to the inside and outside of a beverage bottle.[91] The protective layer consists of starch, oil, vinegar, wheat bran, pineapple fiber, and seaweed. Interestingly, the beverage bottle was made of edible components, namely flour (unknown source), tower powder, shrimp shell powder, food gum, pineapple fiber, alfalfa meal, pomegranate seeds, and many others. However, the prepared edible beverage bottle exhibited a better softening time of 20 h than the bottle made up of starch alone (14–20 h). Therefore, it can be employed in various applications such as tourism, field activities, *etc.*

12. Safety concerns and toxicity of additives used in starch-based edible films and coatings

Food safety and human health are the primary concerns for packaging food products throughout the supply chain. Edible packaging in the form of coatings and films emerges as a novel technique to extend the shelf life of food products. They are convenient, environmentally friendly, and biodegradable. Several active ingredients, including nanoparticles, natural extracts, and essential oils, are usually incorporated into edible films. The active ingredients used to improve the properties of edible packaging films may get released into food matrices by diffusion due to the concertation gradient.[93] Humans can be exposed to any additives, such as nanoparticles and chemicals dissolved in edible packaging films, directly or indirectly.[93,94] Bio-based nanoparticles (*e.g.*, cellulose or chitosan-based) do not impart any health issues; however, it is advisable to avoid inorganic nanoparticles (*e.g.*, ZnO and TiO_2) in the formulation, whose use is debatable. The migration of inorganic nanoparticles into human bodies or the environment requires in-depth researches that are still under way. Testing the possible cytotoxicity of nano-reinforcers employed in active packaging is thus crucial. Most frequently, cell viability upon exposure to nanoparticles in a cell culture or a buffer medium has been used to assess the cytotoxicity of nanoparticles. In several mammalian cell lines, metal oxide nanoparticles have been found to decrease cell viability, cause membrane lipid peroxidation, and harm DNA.[95] Nanoparticles can infiltrate human organs and cause damage due to their microscopic size. They can alter DNA materials, which can lead to genotoxicity. According to studies, nanoparticles such as silver nanoparticles with a size of 20 nm can enter a human lung. Therefore, the quantity and size of the nanoparticles are highly crucial factors when added to edible packaging and must stay below the permitted limit.[96]

Furthermore, minimal toxicity studies are performed to guarantee the safety of additives based on the level of concern.[97] According to studies, the number of essential oils used in food packaging materials is not hazardous and is generally regarded as safe (GRAS).[98] However, higher concentrations of oils may cause allergic and toxicological effects.[99] Furthermore, there are certain drawbacks to employing essential oils as food additives, such as their poor solubility, susceptibility to light, high volatility, and potent odor, which may affect the food's sensory qualities.[96] Additionally, it must be guaranteed that the active

ingredient intended to be added to films and coatings won't change the food product's composition or organoleptic properties.[100]

13. Environmental aspects of starch-based edible films and coatings

Synthetic polymers are extensively used in almost every aspect of life, including packaging, textiles, building materials, and even pharmaceuticals. The global production of plastics decreased by around 0.3% in 2020 compared to 2019 because of the pandemic.[101] Around 80% of the plastic in the sea comes from terrestrial sources, including improper waste management of plastics, sewage, landfill activities near coasts, and trash transported by streams and rivers. Additionally, it is known that trash-derived plastic finds its way into the water. The remaining 20%, however, is made up of garbage produced by ships and boats due to recreational activities, litter discharge, and fishing nets, among other things.[102] Additionally, the contamination of our environment and food supply by plastic particles and other microparticles made of plastic poses a threat to human health. The abundance of synthetic polymers is not only a concern for the environment but also for aquatic animals and human health. Some significant environmental problems include the influence of membrane production on global warming, fossil fuel scarcity, human carcinogenic and non-carcinogenic toxicity, marine ecotoxicity, and potential land use.[103]

It is anticipated that a growing demand for sustainable starch-based biodegradable packaging, including edible films and coatings in food packaging, can reduce substantial greenhouse gas (GHG) emissions, the municipal burden on waste management, and other environmental concerns. According to a study, using biopolymers significantly reduces the use of fossil fuels and positively impacts the environment, such as by lowering carbon dioxide and GHG emissions.[104] In addition, biodegradable polymers have been linked to several environmental benefits. Natural polymers are also used as a long-term fixation for enhancing soil properties, including soil tenacity, soil stabilization, and chemical stabilizing agents, which can boost the productivity of grain yields.[101,105,106] However, care should be taken when using biomolecules in edible packaging to avoid food-borne diseases and ensure human safety.

14. Future perspectives

Inevitably, synthetic plastics offer the most convenience to food manufacturers and consumers for packaging and handling food products, although the current generation is much more aware of the environmental consequences. The foremost challenge for starch-based edible packaging materials could be convincing manufacturers to explore this option. However, the relatively high production costs involved in manufacturing edible packaging materials compared to synthetic plastics remain a challenge. To address this, valorizing or upcycling the agro-food industry waste and discards into valuable food packaging materials is on the rise. For instance, starch isolated from non-conventional sources, including arrowroot starch,[107] lotus rhizome,[108] mango kernels,[109] jackfruit seeds,[17] and loquat seeds[110] has shown potential in film-forming. Therefore, further investigations into non-conventional sources that are not directly consumed by a large fraction of the population could broaden the scope of starch-based edible materials in food packaging applications. Additionally, investigating the effect of novel plasticizers, namely, deep eutectic solvents, can improve the thermo-processibility of starch-based films. The traditional plasticizers used for starch film-forming are glycerol, sorbitol, and other polyols, which tend to migrate into the starch chains and lead to retrogradation during storage time.[111] In contrast, employing natural deep eutectic solvents as green plasticizers exhibits several advantages, including better processability under extrusion conditions,[111] increased starch dissolution and plasticization, resistance to retrogradation,[112] and enhanced film flexibility.[4] However, these green solvents have not been explored in starch-based edible packaging materials so far. Hence, future studies focusing on different combinations (novel sources of starches and plasticizers) with the aim of reducing the production cost and environmental impact with improved function ability and processibility of starch-based packaging materials are essential.

15. Conclusions

The concept of packaging has changed with time, and consumers' demand for nature-derived, sustainable packaging is thriving. Edible packaging is an inexpensive, novel approach for protecting food from numerous hazards while reducing greenhouse gas emissions by replacing single-use plastics in the environment. Reinforcement of bioactive compounds in biopolymers and a nanotechnological approach could successfully improve film properties. Edible films and coatings based on starch are promising; however, they require a significant boost from both the manufacturing and government sectors by providing funding and incentives to conduct further research and achieve the best solution for the environment and circular economy. The incorporation of functional ingredients (*e.g.*, bioactive compounds) and micronutrients (*e.g.*, vitamin D3 and iron) in the formulation could further improve the feasibility of edible packaging and reduce the economic burden on public health systems. Further research should be conducted on the safety of edible packaging, cytotoxicity, and potential for commercial scale-up.

Conflicts of interest

There are no conflicts to declare.

References

1 K. Jogi and R. Bhat, *Sustainable Chem. Pharm.*, 2020, **18**, 100326.
2 R. Santhosh, D. Nath and P. Sarkar, *Trends Food Sci. Technol.*, 2021, **118**, 471–489.

3 J. Liu, Y. Wang, X. Hou, Q. Cui, H. Wu, G. Shen, Q. Luo, S. Li, X. Liu, M. Li, M. Zhou, X. Zhu, A. Chen and Z. Zhang, *LWT*, 2023, **183**, 114930.
4 R. Thakur, V. Gupta, T. Ghosh and A. B. Das, *Food Packag. Shelf Life*, 2022, **33**, 100914.
5 M. C. Gaspar and M. E. Braga, *Curr. Opin. Food Sci.*, 2023, 101006.
6 V. Gupta, R. Thakur, M. Barik and A. B. Das, *J. Agric. Food Res.*, 2023, **11**, 100487.
7 F. M. Pelissari, D. C. Ferreira, L. B. Louzada, F. dos Santos, A. C. Corrêa, F. K. V. Moreira and L. H. Mattoso, *Starches for Food Application*, 2019, pp. 359–420.
8 H. Xu, H. Cheng, D. J. McClements, L. Chen, J. Long and Z. Jin, *Carbohydr. Polym.*, 2022, 119743.
9 S. P. Bangar, W. Scott Whiteside, S. Suri, S. Barua and Y. Phimolsiripol, *Int. J. Food Sci. Technol.*, 2023, **58**, 862–870.
10 L. Zhu, H. Luo, Z.-W. Shi, C.-q. Lin and J. Chen, *Food Chem.: X*, 2023, **17**, 100602.
11 O. Rompothi, P. Pradipasena, K. Tananuwong, A. Somwangthanaroj and T. Janjarasskul, *Carbohydr. Polym.*, 2017, **157**, 748–756.
12 S. Chettri, N. Sharma and A. M. Mohite, *J. Agric. Food Res.*, 2023, **12**, 100615.
13 R. Sharma, N. Gautam, G. Giribabu, R. Kumar and S. Yadav, *Starch/Staerke*, 2023, 2200251.
14 V. Gupta, R. Thakur and A. B. Das, *Int. J. Biol. Macromol.*, 2021, **187**, 575–583.
15 P. Wongphan and N. Harnkarnsujarit, *Int. J. Biol. Macromol.*, 2020, **156**, 80–93.
16 B. Saberi, S. Chockchaisawasdee, J. B. Golding, C. J. Scarlett and C. E. Stathopoulos, *Food Bioprod. Process.*, 2017, **105**, 51–63.
17 R. Santhosh and P. Sarkar, *Food Hydrocolloids*, 2022, **133**, 107917.
18 R. Thakur, B. S. Irom, M. B. Mir, P. Singha, Y. B. Devi, T. Das, R. Ranjan, P. Mishra, B. Naik, V. Kumar and A. K. Gupta, in *Natural Gums*, ed. S. Ahmed and A. Ali, Elsevier, 2023, pp. 373–415, DOI: **10.1016/B978-0-323-99468-2.00014-0**.
19 C. V. Dhumal, J. Ahmed, N. Bandara and P. Sarkar, *Food Packag. Shelf Life*, 2019, **21**, 100380.
20 Y. Zhou, X. Wu, J. Chen and J. He, *Int. J. Biol. Macromol.*, 2021, **184**, 574–583.
21 G. P. Singh, S. P. Bangar, T. Yang, M. Trif, V. Kumar and D. Kumar, *Polymers*, 2022, **14**, 1987.
22 L. Lin, S. Peng, C. Shi, C. Li, Z. Hua and H. Cui, *Int. J. Biol. Macromol.*, 2022, **212**, 155–164.
23 D. Kowalczyk, U. Szymanowska, T. Skrzypek, M. Basiura-Cembala, M. Materska and K. Łupina, *Int. J. Biol. Macromol.*, 2021, **190**, 969–977.
24 A. H. Hashem, M. E. El-Naggar, A. M. Abdelaziz, S. Abdelbary, Y. R. Hassan and M. S. Hasanin, *Int. J. Biol. Macromol.*, 2023, **249**, 126011.
25 F. N. P. De Filmes, *Rev. CIATEC-UPF*, 2021, **13**, 1–9.
26 T. Rahmadi Putri, A. Adhitasari, V. Paramita, M. Endy Yulianto and H. Dwi Ariyanto, *Mater. Today: Proc.*, 2023, **87**, 192–199.
27 A. Kocira, K. Kozłowicz, K. Panasiewicz, M. Staniak, E. Szpunar-Krok and P. Hortyńska, *Agronomy*, 2021, **11**, 813.
28 A. A. Gabriel, A. F. Solikhah and A. Y. Rahmawati, *J. Phys.: Conf. Ser.*, 2021, **1858**, 012028.
29 G. K. Malik, A. Khuntia and J. Mitra, *J. Biosyst. Eng.*, 2022, **47**, 93–105.
30 L. Ballesteros-Mártinez, C. Pérez-Cervera and R. Andrade-Pizarro, *NFS J.*, 2020, **20**, 1–9.
31 K. d. S. Caetano, C. T. Hessel, E. C. Tondo, S. H. Flôres and F. Cladera-Olivera, *J. Food Saf.*, 2017, **37**, e12355.
32 J. Ahmed, R. Santhosh, R. Thakur, M. Mulla and P. Sarkar, *Food Packag. Shelf Life*, 2023, **38**, 101117.
33 K. S. Sandhu, L. Sharma, M. Kaur and R. Kaur, *Int. J. Biol. Macromol.*, 2020, **143**, 704–713.
34 P. C. Nath, S. Debnath, K. Sridhar, B. S. Inbaraj, P. K. Nayak and M. Sharma, *Gels*, 2023, **9**, 1.
35 J. Ahmed, S. B. Dhul and A. Chandak, in *Advances in Food Rheology and Its Applications*, Elsevier, 2023, pp. 517–552.
36 C.-H. Chen, W.-S. Kuo and L.-S. Lai, *Food Hydrocolloids*, 2009, **23**, 2132–2140.
37 D. Peressini, B. Bravin, R. Lapasin, C. Rizzotti and A. Sensidoni, *J. Food Eng.*, 2003, **59**, 25–32.
38 V. Sharma, M. Kaur, K. S. Sandhu and S. K. Godara, *Int. J. Biol. Macromol.*, 2020, **159**, 243–249.
39 L. Zhang, J. Zhao, Y. Zhang, F. Li, X. Jiao and Q. Li, *Int. J. Biol. Macromol.*, 2021, **192**, 444–451.
40 P. Pająk, D. Gałkowska, L. Juszczak and G. Khachatryan, *Food Packag. Shelf Life*, 2022, **34**, 100995.
41 S. S. N. Chakravartula, R. V. Lourenço, F. Balestra, A. M. Q. B. Bittante, P. J. do Amaral Sobral and M. Dalla Rosa, *Food Packag. Shelf Life*, 2020, **24**, 100498.
42 P. R. Fitch-Vargas, E. Aguilar-Palazuelos, J. de Jesús Zazueta-Morales, M. O. Vega-García, J. E. Valdez-Morales, F. Martínez-Bustos and N. Jacobo-Valenzuela, *J. Food Sci.*, 2016, **81**, E2224–E2232.
43 L. P. Wigati, A. A. Wardana, F. Tanaka and F. Tanaka, *Food Packag. Shelf Life*, 2023, **35**, 101010.
44 G. Zuo, X. Song, F. Chen and Z. Shen, *J. Saudi Soc. Agric. Sci.*, 2019, **18**, 324–331.
45 H. Wu, T. Li, L. Peng, J. Wang, Y. Lei, S. Li, Q. Li, X. Yuan, M. Zhou and Z. Zhang, *Food Hydrocolloids*, 2023, **139**, 108509.
46 A. A. Abdillah and A. L. Charles, *Int. J. Biol. Macromol.*, 2021, **191**, 618–626.
47 S. Punia Bangar, K. S. Sandhu, A. V. Rusu, P. Kaur, S. S. Purewal, M. Kaur, N. Kaur and M. Trif, *Coatings*, 2021, **11**, 1167.
48 H. Wu, Y. Lei, J. Lu, R. Zhu, D. Xiao, C. Jiao, R. Xia, Z. Zhang, G. Shen and Y. Liu, *Food Hydrocolloids*, 2019, **97**, 105208.
49 C. M. Chandrasekar, H. Krishnamachari, S. Farris and D. Romano, *Carbohydr. Polym. Technol. Appl.*, 2023, **5**, 100328.
50 H. Wu, J. Wang, T. Li, Y. Lei, L. Peng, J. Chang, S. Li, X. Yuan, M. Zhou and Z. Zhang, *Int. J. Biol. Macromol.*, 2023, **240**, 124444.
51 M. Pirouzifard, R. A. Yorghanlu and S. Pirsa, *J. Thermoplast. Compos. Mater.*, 2020, **33**, 915–937.

52 J. G. de Oliveira Filho, B. R. Albiero, L. Cipriano, C. C. de Oliveira Nobre Bezerra, F. C. A. Oldoni, M. B. Egea, H. M. C. de Azeredo and M. D. Ferreira, *Cellulose*, 2021, **28**, 6499–6511.
53 N. Chen, H.-X. Gao, Q. He and W.-C. Zeng, *Food Struct.*, 2023, **36**, 100318.
54 Z. Song, J. Wei, Y. Cao, Q. Yu and L. Han, *Food Chem.*, 2023, **418**, 135958.
55 Y. Shen, J. Zhou, C. Yang, Y. Chen, Y. Yang, C. Zhou, L. Wang, G. Xia, X. Yu and H. Yang, *Int. J. Biol. Macromol.*, 2022, **212**, 20–30.
56 M. Hasan, R. Rusman, I. Khaldun, L. Ardana, M. Mudatsir and H. Fansuri, *Int. J. Biol. Macromol.*, 2020, **163**, 766–775.
57 R. Thakur, B. Saberi, P. Pristijono, J. Golding, C. Stathopoulos, C. Scarlett, M. Bowyer and Q. Vuong, *Int. J. Biol. Macromol.*, 2016, **93**, 952–960.
58 S. Yao, B.-J. Wang and Y.-M. Weng, *Food Packag. Shelf Life*, 2022, **32**, 100845.
59 P. G. Seligra, C. M. Jaramillo, L. Famá and S. Goyanes, *Carbohydr. Polym.*, 2016, **138**, 66–74.
60 E. Chavez-Marquez, M. S. B. Bernedo, E. M. de Jara, M. J. Quequezana-Bedregal, E. E. Gutierrez-Oppe and P. d. A. Pessôa Filho, *Int. J. Biol. Macromol.*, 2023, **242**, 125080.
61 E. Malekzadeh, A. Tatari and M. D. Firouzabadi, *Carbohydr. Polym.*, 2023, **309**, 120699.
62 T. Ghosh and V. Katiyar, *Int. J. Biol. Macromol.*, 2022, **211**, 116–127.
63 G. Ghoshal and M. Kaur, *Food Chem. Adv.*, 2023, **3**, 100356.
64 S. B. Dhull, S. P. Bangar, R. Deswal, P. Dhandhi, M. Kumar, M. Trif and A. Rusu, *Foods*, 2021, **10**, 3097.
65 D. Lourdin, H. Bizot and P. Colonna, *Macromol. Symp.*, 1997, **114**, 179–185.
66 C. Arismendi, S. Chillo, A. Conte, M. A. Del Nobile, S. Flores and L. N. Gerschenson, *LWT–Food Sci. Technol.*, 2013, **53**, 290–296.
67 P. B. Wilfer, G. Giridaran, J. J. Jeevahan, G. B. Joseph, G. S. Kumar and N. J. Thykattuserry, *Mater. Today: Proc.*, 2021, **44**, 3903–3907.
68 Y. Li, F. Wang, J. Xu, T. Wang, J. Zhan, R. Ma and Y. Tian, *Food Hydrocolloids*, 2023, **137**, 108405.
69 H. Ren, Z. Xu, C. Du, Z. Ling, W. Yang, L. Pan, Y. Tian, W. Fan and Y. Zheng, *Int. J. Biol. Macromol.*, 2023, **242**, 124938.
70 J. Ahmed, M. Mulla and Y. A. Arfat, *Food Control*, 2017, **78**, 160–168.
71 L. T. Sanchez, M. I. Pinzon and C. C. Villa, *Food Chem.*, 2022, **371**, 131121.
72 A. Nikmanesh, H. Baghaei and A. Mohammadi Nafchi, *Foods*, 2023, **12**, 2955.
73 V. Sharma, M. Kaur, K. S. Sandhu and S. K. Godara, *Int. J. Biol. Macromol.*, 2020, **159**, 243–249.
74 L. Zhang, J. Zhao, Y. Zhang, F. Li, X. Jiao and Q. Li, *Int. J. Biol. Macromol.*, 2021, **192**, 444–451.
75 C. Ma, C. Tan, J. Xie, F. Yuan, H. Tao, L. Guo, B. Cui, C. Yuan, W. Gao, F. Zou, Z. Wu, P. Liu and L. Lu, *Int. J. Biol. Macromol.*, 2023, **242**, 124914.
76 N. Ardjoum, N. Chibani, S. Shankar, S. Salmieri, H. Djidjelli and M. Lacroix, *Int. J. Biol. Macromol.*, 2023, **224**, 578–583.
77 Z. Zong, M. Liu, H. Chen, M. A. Farag, W. Wu, X. Fang, B. Niu and H. Gao, *Food Chem.*, 2023, **405**, 134839.
78 B. Ghanbarzadeh, H. Almasi and A. A. Entezami, *Ind. Crops Prod.*, 2011, **33**, 229–235.
79 B. Saberi, Q. V. Vuong, S. Chockchaisawasdee, J. B. Golding, C. J. Scarlett and C. E. Stathopoulos, *Food Bioprocess Technol.*, 2017, **10**, 2240–2250.
80 M. A. Bertuzzi, E. F. Castro Vidaurre, M. Armada and J. C. Gottifredi, *J. Food Eng.*, 2007, **80**, 972–978.
81 F. C. Feng Wentian, *CN Pat.*, CN107011544A, 2017.
82 W. Zhongliang, *CN Pat.*, CN108250493A, 2018.
83 J. S. He Wanchen, G. Mou, T. Yanfeng, Q. Fang, and X. Zhu, *CN Pat.,* CN111808333A, 2020.
84 T. L. Yu Zan, Z. Wen, Z. Luo, Y. Zhang, W. Xuexue, and J. Du, *CN Pat.,* CN108752645A, 2018.
85 C. J. Long zhu, *CN Pat.*, CN109438772B, 2018.
86 Z. Guquan, *CN Pat.*, CN109294000A, 2018.
87 Y. F. Bo Cui, L. Guo, B. Yu, C. Yuan, and Y. Zou, *CN Pat.*, AU2019271993B2, 2021.
88 L. F. Lu Chengwen, T. Zhang, X. Yan, S. Mao, and X. Zhou, *CN Pat.*, CN114736436A, 2022.
89 L. Hefei Xu Ya New Mstar Technology, *CN Pat.*, CN109054105A, 2018.
90 M. E. Wright, *WO Pat.*, WO2020018480A1, 2019.
91 C. Y. Cao Shengzhu, and J. Zhu, *CN Pat.*, CN110817089A, 2019.
92 L. J. Lee Youngjae, *KR Pat.*, KR102261416B1, 2020.
93 L. Kumar, D. Ramakanth, K. Akhila and K. K. Gaikwad, *Environ. Chem. Lett.*, 2022, **20**, 875–900.
94 M. V. Nikolic, Z. Z. Vasiljevic, S. Auger and J. Vidic, *Trends Food Sci. Technol.*, 2021, **116**, 655–668.
95 S. C. Sahu and A. W. Hayes, *Toxicol. Res. Appl.*, 2017, **1**, DOI: 10.1177/2397847317726352.
96 J. Kaur, J. Singh, P. Rasane, P. Gupta, S. Kaur, N. Sharma and D. Sowdhanya, *Food Biosci.*, 2023, **53**, 102689.
97 S. C. Lourenço, M. Moldão-Martins and V. D. J. M. Alves, 2019, **24**, 4132.
98 L. Motelica, D. Ficai, A. Ficai, O. C. Oprea, D. A. Kaya and E. J. F. Andronescu, *Foods*, 2020, **9**, 1438.
99 J. Jeya Jeevahan, M. Chandrasekaran, S. P. Venkatesan, V. Sriram, G. Britto Joseph, G. Mageshwaran and R. B. Durairaj, *Trends Food Sci. Technol.*, 2020, **100**, 210–222.
100 D. Dutta and N. Sit, *J. Food Sci. Technol.*, 2023, **60**, 1888–1902.
101 R. K. Gupta, P. Guha and P. P. Srivastav, *Food Chem. Adv.*, 2022, **1**, 100135.
102 A. G. Kumar, K. Anjana, M. Hinduja, K. Sujitha and G. Dharani, *Mar. Pollut. Bull.*, 2020, **150**, 110733.
103 P. Yadav, N. Ismail, M. Essalhi, M. Tysklind, D. Athanassiadis and N. Tavajohi, *J. Membr. Sci.*, 2021, **622**, 118987.
104 J. W. Gooch, in *Encyclopedic Dictionary of Polymers*, ed. J. W. Gooch, Springer New York, New York, NY, 2011, pp. 479–479, DOI: 10.1007/978-1-4419-6247-8_7797.

105 W. Che, J. Liu, H. Li, C. He, Y. Bai, Z. Song, Y. Wang, W. Qian and Z. Chen, *Bull. Eng. Geol. Environ.*, 2021, **81**, 22.
106 A. Soldo, M. Miletić and M. L. Auad, *Sci. Rep.*, 2020, **10**, 267.
107 J. G. de Oliveira Filho, C. C. d. O. N. Bezerra, B. R. Albiero, F. C. A. Oldoni, M. Miranda, M. B. Egea, H. M. C. de Azeredo and M. D. Ferreira, *Food Packag. Shelf Life*, 2020, **26**, 100589.
108 S. Sukhija, S. Singh and C. S. Riar, *Food Hydrocolloids*, 2016, **60**, 128–137.
109 A. Nawab, F. Alam, M. A. Haq, Z. Lutfi and A. Hasnain, *Int. J. Biol. Macromol.*, 2017, **98**, 869–876.
110 T. L. Cao and K. B. Song, *Food Hydrocolloids*, 2019, **97**, 105198.
111 M. Zdanowicz, *Carbohydr. Polym.*, 2020, **229**, 115574.
112 M. Zdanowicz, T. Spychaj and H. Mąka, *Carbohydr. Polym.*, 2016, **140**, 416–423.